Functionalized Masks: Powerful Materials against COVID-19 and Future Pandemics

Farzad Seidi,* Chao Deng, Yajie Zhong, Yuqian Liu, Yang Huang, Chengcheng Li, and Huining Xiao*

The outbreak of COVID-19 revealed the vulnerability of commercially available face masks. Without having antibacterial/antiviral activities, the current masks act only as filtering materials of the aerosols containing microorganisms. Meanwhile, in surgical masks, the viral and bacterial filtration highly depends on the electrostatic charges of masks. These electrostatic charges disappear after 8 h, which leads to a significant decline in filtration efficiency. Therefore, to enhance the masks' protection performance, fabrication of innovative masks with more advanced functions is in urgent demand. This review summarizes the various functionalizing agents which can endow four important functions in the masks including i) boosting the antimicrobial and self-disinfectant characteristics via incorporating metal nanoparticles or photosensitizers, ii) increasing the self-cleaning by inserting superhydrophobic materials such as graphenes and alkyl silanes, iii) creating photo/electrothermal properties by forming graphene and metal thin films within the masks, and iv) incorporating triboelectric nanogenerators among the friction layers of masks to stabilize the electrostatic charges and facilitating the recharging of masks. The strategies for creating these properties toward the functionalized masks are discussed in detail. The effectiveness and limitation of each method in generating the desired properties are well-explained along with addressing the prospects for the future development of masks.

1. Introduction

The enormous impact of COVID-19 pandemic on the global economy and health has stimulated extensive researches including material-related ones to address the urgent issues associated with this highly transmittable disease. The origin of this new pandemic is a new type of coronavirus named as severe acute respiratory syndrome coronavirus 2 (SARS-CoV-2), which raises significant threat to human beings.[1,2] The high transmission rate of this virus and its strong resistance against various types of antiviral and disinfecting agents has led to a new dilemma worldwide.[3,4] In less than one year, almost all counties around the world have been infected by SARS-CoV-2. Some tough measures such as travel restrictions,[5] shutting down of schools and business and even the lockdown of the entire city[6] were introduced at the initial wave to prevent more spreading of this deadly virus; whereas the consequences remain as one of the largest disasters in human history.[7,8]

While several vaccines have been announced to be effective in preventing of this virus,[9–11] vaccination of the entire population worldwide requires a prolonged period of time or could be even impossible. Meanwhile, SARS-CoV-2 has constantly changed through mutation, thus creating new variants which are highly infectious with worse fatality rates and also potentially lowering the effectiveness of vaccination.[12] Multiple variants of coronavirus have been reported in several countries over the past months during this pandemic.[13] Therefore, protection of the respiratory system is the simplest and the most convenient strategy to avoid infection and to minimize viral spreading. New studies have shown that surgical face masks can effectively inhibit the transferring of infecting agents, bacteria, and viruses from the environment to the human body.[14,15] However, there are several significant limitations related to the common face masks such as nonreusability and lack of antibacterial and antiviral activities. Therefore, it is necessary to replace the mask with a new one after use for a short period particularly in high risk regions, which leads to the generation of an enormous amount of waste masks. On the one hand, the discarded masks may contain a high number of microorganisms and viruses that could be coronavirus hazards and increase the high risk of the secondary transmission of disease,[16] thereby raising the high demand for the safe disposal of the used masks. On the other hand, the worldwide consumption of face masks is over 200 million pieces per day,[17] which creates a huge amount

Prof. F. Seidi, Dr. C. Deng, Y. Zhong, Prof. Y. Liu, Prof. Y. Huang, Prof. C. Li
Jiangsu Co-Innovation Center of Efficient Processing and Utilization of Forest Resources and International Innovation Center for Forest Chemicals and Materials
Nanjing Forestry University
Nanjing 210037, China
E-mail: f_seidi@njfu.edu.cn
Prof. H. Xiao
Department of Chemical Engineering
University of New Brunswick
Fredericton, New Brunswick E3B 5A3, Canada
E-mail: hxiao@unb.ca

The ORCID identification number(s) for the author(s) of this article can be found under https://doi.org/10.1002/smll.202102453.

of plastic waste since the majority of face masks is based on nonwoven fabrics from non-biodegradable polypropylene (PP). Currently, most countries use incineration as a key method for the disposing of discarded masks, which, however, produces a high amount of toxic gases and increases the greenhouse effect due to the substantial amount of CO_2 released.[18,19] Therefore, it is in high demand to increase the efficiency, lifetime, and reusability of face masks for better protection and meanwhile minimizing the negative environmental impacts.

To reuse the commercially available surgical face masks, washing with detergents or decontamination with disinfectant agents has been attempted, which, however, can reduce the efficiencies of the mask. For instance, washing the N95 masks with ethanol can destroy the fibrous structure of the PP layer in the mask.[20] Decontamination of N95 masks using H_2O_2 vapor,[21] H_2O_2 plasma,[22] ozone,[23] heating at 85 °C under various humidity levels,[24,25] and dry heat pasteurization[26] have been proved as proper methods for mask disinfection. The remaining disinfectant agent even at a trace amount might cause toxic effects on the human body. Therefore, for long-term use, the disinfection of the masks using external agents is not a recommended method.[27] Furthermore, it has been reported that various decontamination methods can vanish the charge of the PP layer in face masks leading to a significant reduction in the filtration efficiencies. While recharging of the masks usually requires high-tech method, Hossein et al. reported a simple method by using 1 kV potential through a DC voltage generator for successfully recharging the decontaminated N95 masks.[28] However, all these methods for decontamination and recharging require special equipment and skills which limit their practical utilization, particularly in remote areas.

Based on what explained above, the functionalization and engineering of the face masks for improving their inherent efficiencies and reusability without external cleaning and disinfectant agents are crucial matter not only for urgent need currently but also for future pandemics. Functionalization of masks has been performed to endow the following properties in the mask: i) increasing the anti-microbial and self-disinfecting properties by incorporating well-known antimicrobial agents such as metal nanoparticles (Ag, CuO, ZnO, etc.) and photosensitizers, ii) improving the self-cleaning behavior of the masks by superhydrophobization of the mask surface via the incorporation of graphenes, alkyl silanes, and perfluorinated polymers, iii) increasing the photothermal and electrothermal property of the mask for generation of high local temperatures that can easily inactivate a broad spectrum of bacteria and viruses, and iv) increasing the long-term stability of the static charges of inner layer in the masks along with improving the rechargeability of masks by incorporating triboelectric nanogenerators (TENGs) between the friction layers of the masks.

In this review, we first provide a brief discussion about the interactions of SARS-CoV-2 with various surfaces and the lifetime of this virus on the different surfaces in response to various disinfectant agents. After introducing the common properties of the face masks commonly used nowadays, we provide a real-time and appropriate summary of research works related to face masks from both modification and application

points of view. As far as we know, this is the first comprehensive review detailing and summarizing the functional modification of the masks, which addresses the urgent needs under the currently ongoing pandemic. The methods for the preparation of the functional masks have been explained in detail and various functions that affect the efficiencies of the modification method have been discussed. Furthermore, the impact of the functionalization method on the antiviral, antibacterial, self-cleaning, and self-sterilization of the masks have been discussed in detail. The findings summarized herein could provide guidance for the further exploration of the functionality of the face masks for a variety of applications.

2. Surface Stabilities and Decontamination of SARS-CoV-2

The SARS-CoV-2 is a spherical shape enveloped virus with the size of around 120 nm (**Figure 1**).[29] This virus is made of three main components: RNA genome, lipidbilayer membrane, and surface proteins. The surface proteins are including spike (S) glycoprotein, membrane (M) protein, and small envelope (E) protein. Better understanding about this virus and the role of each protein is beneficial to the selection of proper materials for inactivating the corresponding action. S protein is responsible for receptor binding and membrane fusion. The lipide membrane protects the RNA of the virus which then can be replicated after entering the cells. The most abundant surface protein is the M protein whose main role is to control the virus assembly.[30] Finally, E protein is the smallest surface protein that controls the virus assembly, envelope formation, and permeability of the membrane.[31]

It has been proved that the inanimate surface contact is one of the key routes of the indirect transmission of SARS-CoV-2.[33] The lifetime and stability of SARS-CoV-2 and other coronaviruses on different surfaces have been reviewed by several groups.[34,35] The stability of SARS-CoV-2 on surfaces is somehow similar to SARS-CoV-1.[36] Indeed, the SARS-CoV-2 remains viable on some surfaces such as plastic and stainless steel up to 72 h, whereas on the copper and cardboard surfaces no viable virus was detected after 4 and 24 h, respectively.[36,37] The surfaces were free of the virus for high-pressure laminate, rubber flooring, wood laminate floor, commercial carpet after 8 h, vinyl sheet after 12 h, acrylic surface and quartz surface after 30 h, and vinyl wall covering after 168 h.[37] The reason for the different lifetimes of viruses on various surfaces is related to the different interactions of each surface with the virus, leading to the different time periods for inactivation.

The possible mechanisms for inactivation of SARS-CoV-2 by antiviral drugs,[38] disinfectants,[39] and various surfaces[34,40,41] have been reviewed already. Alcohols (ethanol and isopropanol) kill and inactivate the coronavirus via dissolving the virus lipid membrane, damaging its RNA strain, and denaturation of its proteins probably through disrupting the intramolecular H-bondings.[39] Various oxidizing agents (peroxides, peracids, ozone, etc.) can deactivate the enveloped viruses via the oxidation of thiol groups in virus proteins and denaturation of proteins.[42–45] Similarly, iodophors can release iodine which can penetrate into the membrane and oxidize the proteins' thiols
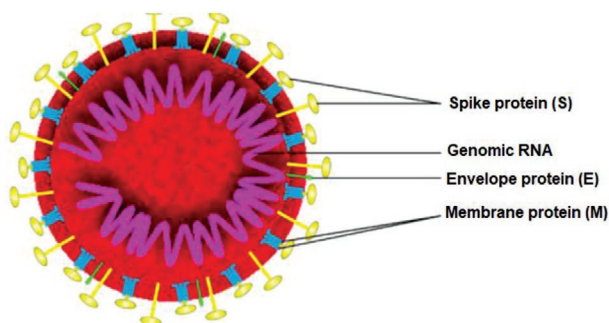
ADVANCED
SCIENCE NEWS
www.advancedsciencenews.com

NANO · MICRO
small
www.small-journal.com

Figure 1. General architecture of SARS-CoV-2. Reproduced with permission.[32] Copyright 2020, MDPI.

and also damage the RNA of the virus. Therefore, tethering of the safe oxidizing agents on the surface of personal protection equipment (PPE) can be used as an appropriate approach for fabrication of antiviral PPEs. Various phenolic-based disinfectants (including essential oils) kill the viruses via damaging the membrane of the virus which leads to the leakage of the seepage of the intracellular components of the virus and denaturation of proteins. In general, detergents or surfactants are amphiphiles with similar structures to the lipid molecules in the lipid bilayer of the virus. Therefore, these surfactants can create strong interaction with lipids in the virus membrane and tear down the lipid membrane.[41,46] Overall, all the surfaces have been categorized into three groups including natural surfaces, artificial surfaces, and biomimetic surfaces.[34,40,41] Natural surfaces containing some natural herbs and natural extracts can damage the RNA of the virus, and also inhibit the construction of enzymes for virus replication. In the artificial surfaces, the inactivation mechanisms have been divided into three forms including direct disinfection, indirect disinfection, and receptor inactivation. Surfaces containing some materials such as silver and copper have direct antiviral properties by releasing low concentrations of Ag^+, Cu^+, and Cu^{2+} ions which can prevent the proliferation of the virus via inhibiting the activity of respiratory enzymes and obstructing the functions of virus' RNA.[47] For indirect inactivation, several mechanisms have been proposed. i) The surfaces producing heat, light, and free radicals by responding to an external trigger can inactivate the virus. For instance, nanoparticles of some metals such as Au, Cu, and Ag can generate the localized surface plasmon resonance upon visible illumination.[48] ii) Some materials such as graphene[49] and Au[50] have photothermal properties which create high temperatures upon illumination with sunlight. The high temperature can inactivate various types of viruses including SARS-CoV-2.[51] iii) The materials such as photosensitizers and semiconductors can produce free radicals which are the well-known agents for inactivating viruses and other microorganisms. iv) There is another group of antiviral nanomaterials (cerium oxide, tungsten oxide, etc.) that act by inducing the redox reactions between the surface with the virus.[52] v) Some surfaces bear small molecules with the ability to capture the virus and passivation of its spikes receptors. Smith and Smith listed 77 small molecules with the ability to attach the S-protein of SARS-CoV-2 and inactivate it.[53] Immobilization of these small molecules on the surface of masks can improve the antiviral

properties of the masks.[54] The biomimetic surfaces often play the role based on the self-cleaning strategy. Excellent progress has been reported on developing bioinspired superhydrophobic surfaces by mimicking nature.[55,56]

As it is obvious from the above examples, nanotechnology can be utilized as a proper tool for fighting against SARS-CoV-2. Several review papers have been published on the possible roles of nanomaterials for combating the current pandemic.[57–59] Indeed, the first vaccine that went to the clinical trials was an mRNA vaccine tethered on lipid nanoparticles.[60] Improving the efficacy of PPE and fabrication of synergistic antiviral coatings and surfaces is still of critical importance in reducing the spreading of this virus. In the case of face masks, tethering of the above-mentioned disinfectants and nanomaterials on the surface of the masks can improve the antiviral properties of the surface and therefore, prevent the indirect spreading and transmitting of SARS-CoV-2.

3. Face Masks

Face masks are the simple protection tools for fighting pandemics by preventing the wide spreading of viruses and microorganisms, trapping them and in advanced cases inactivating the trapped viruses/bacteria. Various types of face masks that can be applied for protection against COVID-19 have been reviewed by several groups.[61–63] Various types of commonly used face masks during the COVID-19 pandemic are depicted in **Figure 2**.

The compressed polyurethane (PU) foam mask generally has a 3D porous structure with the ability to block 99% of the pollen-sized particles, which is cost-effective and washable. However, it almost has no filtration effect against small-size microorganisms including bacteria and viruses. Cloth face masks are a kind of simple homemade masks fabricated from a piece of household fabrics including cotton, woven, felted, knitted, and so on.[64,65] These masks are usually washable and can be applied several times. The filtration efficiency of these masks depends on the type and structure of the fabrics and also the number of utilized cloth layers for the mask. However, they offer weak filtration efficiencies for viruses.

Figure 2. Commonly used face masks against COVID-19 pandemic.

Surgical face masks made from polypropylene (PP) are the most popular ones world-wide. The masks generally consist of a PP meltblown nonwoven sandwiched between two regular PP nonwoven fabrics.[66] The central layer is the main layer for filteration and the role of the inner and outer layers are, respectively, for absorbing moisture and repelling the water. While a surgical mask is very effective in filtration of aerosols and large particles (>5 μm), it does not offer good filtration for very small particles including viruses. Additionally, these non-biodegrable PP masks are the main reason for plastic pollution during the current pandemic. Filtering facepiece respirators (FFRs) are a group of face masks with the ability to filter very small particles even as small as 20 nm in some cases.[66] Various types of FFRs including N95, N99, KN95, P100, FFP2, and FFP3 are available and named according to different standards of different countries. The number usually shows the filtration efficiencies. For instance, N95 and N99 can filter, respectively, 95% and 99% of airborne particles. The N95 respirator, the most famous FFR during the COVID-19 pandemic, is known as an electret filter because it bears an electrocharged layer with the ability to trap the microaerosol droplets, virions, and various microorganisms with sizes larger than 100 nm.[67,68] The KN95 respirator is made of four layers including the outer/inner layers, a filter layer, and a cotton layer.[69] While the efficiencies of N95 and KN95 have been reported to be somehow similar, but the filter layer of KN95 is around 8-times thinner than N95.[69] The filtration effectiveness of 0.3 μm particles by FFP1, FFP2, and FFP3 are around 80%, 94%, and 99%, respectively.[70] Practically, the filtration efficiency of FFP2 and FFP3 is almost equal to N95 and N99, respectively.

It is noteworthy to mention that the efficiency of the masks with the same name but fabricated by different companies could be different. Therefore, the performances and filtration efficiencies aforementioned should be considered as approximate values.

4. Modification of Masks

The various strategies that have been explored for the functionalization of masks are summarized in **Table 1**, in which the active effect is classified by the species along with modification methods. The goals of these strategies are to improve the reusability, lifetime, antimicrobial activity, and self-decontamination of the masks. In the following sections the descriptions regarding each strategy in detail are presented in terms of the type of the active species incorporated into the masks.

4.1. Metals and Salts

Various metals and salts, especially in their nanostates, have been reported as strong antimicrobial agents.[97] The most well-developed antimicrobial metals for biomedical applications include silver,[98,99] copper,[100,101] and zinc.[102,103] There are a number of reports regarding the fabrication of antimicrobial fabrics by embedding such metals into the fabrics structures, such as Ag nanoparticles (NPs)[104] and Ag nanowires (NWs)[105]

coated onto cotton fabrics, CuO-impregnated woven and non-woven fabrics[106] and Ag/ZnO-embedded cotton/polyester blend fabrics.[107] Especially, there are new reports about the efficiency of metal nanoparticles for inactivating SARS-CoV-2 such as Ag NPs,[108] copper,[109,110] and zinc ions.[111] Accordingly, these metals in various forms have been embedded in the structures of respiratory face masks to endow the masks with boosted antimicrobial/antiviral activity.

In the simplest strategy, the PP middle layer of surgical masks was coated with various types of salts (including NaCl, K_2SO_4, and KCl) in the presence of surfactants to provide antiviral activity.[71,72] This coating enhanced the hydrophilicity of the PP layer (**Figure 3**a) which is helpful in the adsorption of viral aerosols. While bare PP filter showed no resistance against the penetration of H1N1 virus-containing aerosol (2.5–4 μm), coating with NaCl enhanced the filtration efficiency up to 85% with increasing the NaCl content (Figure 3b).[71] The adsorbed viruses could be deactivated in a two-step process: i) adsorption of the viral aerosol on PP surface along with dissolving the salt in the aerosols, ii) gradual evaporation of water which induces supersaturation and then recrystallization of salt. Consequently, the walls of the cell hosting virus are damaged by increasing the osmotic pressure of the outside medium during the drying process of the aerosol. The hemagglutinin activity (HA), a criteria for in vitro virus stability, showed a reduction of around 8% for bare PP filter; whereas it was reduced by almost 100% for NaCl-coated PP filter (Figure 3c).[71] Also, TEM images revealed morphological destruction of influenza virus by NaCl-coated PP, leading to a nonspherical shape. Similarly, the PP layers coated with NaCl, K_2SO_4, or KCl could inactivate both Gram-positive and Gram-negative bacterial aerosols in vitro upon salt recrystallization.[72]

Silver as a strong antimicrobial agent was used in 2006 by Li et al. for the fabrication of antibacterial masks.[73] In this report, the most hydrophobic outer surface of surgical masks was coated with composite nanoparticles composed of Al_2O_3, TiO_2, and Ag(I). Incubation of the NPs-coated masks in bacterial medium for 48 h showed 100% inhibition in viable *Escherichia coli* and *Staphylococcus aureus* whereas for the pristine mask no inhibition was reported. Instead, around 25% and 50% increases in the viable counts were reported for *E. coli* and *S. aureus*, respectively. Additionally, the as-modified mask showed no skin inflammation, itchiness, and allergy on 20 volunteers who wore the mask. Similarly, simple soaking of entire face masks in a dispersion of starch-capped Ag NPs yielded functional face masks with strong antimicrobial efficiency.[74] The size control of Ag NPs is critical to maintain the strong antibacterial efficiency. This is mainly due to the fact that the size must be sufficiently small to allow nanomaterials to cross the cell wall of bacteria, thereby inducing destructive effects on the cell wall and DNA. The OH groups of starch cover the surface of Ag NPs and prevent the flocculation of nanoparticles. The zone inhibition diameters for the modified mask after soaking in 50 and 100 ppm of Ag NPs were increased around 1.5 and 2.1 times for *S. aureus* and around 2.0 and 4.3 times for *E. coli*. However, since the Ag NPs are covered in the whole structure of this mask, evaluation of the cytotoxicity of the mask should an important issue which, unfortunately, was ignored by the corresponding researchers.

Table 1. Strategies for the fabrication of functionalized masks with improved performance.

Mask's modification method	Active effect	Remarks of the modified mask	Ref.
Metals and salts			
Coating the PP layer with various types of salts (NaCl, K_2SO_4, and KCl)	Increasing effect of the salts on the osmotic pressure of aerosols of viruses	1) Increasing the filtration efficiency 2) Inactivating Gram-positive and Gram-negative bacteria	[71,72]
Coating the outer most hydrophobic surface of surgical masks with $Al_2O_3/TiO_2/Ag(I)$ NPs	Biocidal effect of Ag(I)	1) 100% inhibition of *E. coli* and *S. aureus* in 48 h 2) No skin inflammation, itchiness, and allergy on 20 volunteers	[73]
Dip coating the whole face mask by starch capped Ag NPs	Biocidal effect of Ag(I)	Increasing the zone inhibition diameters up to 2.1 and 4.3 times for *S. aureus* and *E. coli*, respectively	[74]
Developing new mask using PAN/Ag nano-fibers composite membrane	Biocidal effect of Ag(I)	1) High stability of Ag on the fabrics 2) Inactivation of *Pseudomonas* and *Staphylococcus* bacteria	[75]
Developing new mask using CuO-loaded PAN nanofibers	Biocidal effect of CuO	1) High antibacterial activity against *E. coli* and *B. subtilis* 2) At high contents of CuO, showed cytotoxicity	[76]
Coating the surface of PP layer with shellac/CuNPs nanocomposite	1) Photoactive and hydrophobic effect of shellac 2) Biocidal effect of Cu NPs 3) Plasmonic effect of Cu NPs	1) Increase the WCA of the PP to 143° 2) Increase the T of mask to >70 °C under sun irradiation 3) Inactivation of *E. coli* (>99.99%) under sun irradiation	[77]
Developing new mask composed of PA66 layer embedded with Zn(II) ions	1) Capturing the virus by PA66 2) Killing the virus by Zn(II)	1) Higher washability than cotton 2) Higher virus capturing than PP 3) Around 2-log reduction in IAV and SARS-CoV-2 titers in 1 h	[78]
Dip coating of PP in Cu@ZIF-8 NWs dispersion	Biocidal effect of Cu(II) and Zn(II)	Keep the hydrophobicity of PP Improved filtration efficiency Highly biocompatible (cell viability >99% in 48 h) Inhibition of *E. coli* (>90%), *S. mutans* (>85%) and SARS-CoV-2 (55%)	[79]
Photosensitizers			
Proposing utilizing photoactive conjugated polymers and oligomers in masks structure	Release of biocidal ROS	100% inactivating of SARS-CoV-2 near-UV light irradiation	[80]
Grafting the cationic poly(DEAE) onto the cotton fibers following by tethering with anionic photosensitizers	Release of biocidal ROS	Kill >99.99% *E. coli* and *L. innocua and* inactivating of T7 bacteriophage virus under light exposure	[81]
Developing new masks using photocatalytic TiO_2 based filters	Release of biocidal ROS	Kill all *E. coli* in 1 min under UV light (365 nm) Applied for the fabrication of light sterilizable masks	[82]
Graphenes			
Embedding GO-crosslinked by TAIC into the cotton fabrics		Inhibition (>99%) against *E. coli* and *B. subtilis* No irritation to rabbit skin Complete inhibition against SARS-CoV-2 viral	[83,84]
Embedding a layer of PVDF/GO on the PP layer	1) Superhydrophobicity of PVDF 2) 2)TENG rule of GO NPs	1) Increase the hydrophobicity of the PP 2) Increased the charge on PP to 2.0 nC cm^{-2} 3) Long-term charge retention (5 days) 4) Recovery electrostatic charges of mask by simple thumb pressing	[85]
Incorporation of rGO into the melt-blown nonwoven fabrics	High electrothermal effect of rGO	1) Rise local T to 80 °C in 4 min at voltage 3 V 2) Rise local T to 72 °C under sunlight 3) Kill >99% *E. coli* in 15 min upon electrifying 4) No effect on air permeability and filtration efficiency	[86]
Immobilization of LIG on the surface of surgical mask	High hydrophobicity and photothermal activity of the laser-induced graphene	1) Superhydrophobicity of the modified mask (WCA 140°) 2) 95% absorption of solar spectrum 3) Increasing the surface temperature of mask to 80 °C in 100 s	[87]
Immobilization of LIG/Ag composite on the surface of N95 mask	1) Biocidal and plasmonic effect of Ag(I) 2) High hydrophobicity and photothermal activity of the 3) laser-induced graphene	1) Superhydrophobicity of the modified mask (WCA 140°) 2) 100% absorption of solar spectrum 3) Increasing the surface temperature of mask to 80 °C in 60 s	[88]
Immobilization of LIG on the surface of surgical mask	High hydrophobicity and photothermal activity of the laser-induced graphene	1) Superhydrophobicity of the modified mask (WCA 150°) 2) Increasing the surface T of mask to 62 °C in 60 s in solar irradiation 3) Killing >99.99% of *E. coli* upon electrifying the mask upon solar irradiation	[89]

ADVANCED
SCIENCE NEWS

www.advancedsciencenews.com

NANO · MICRO

small

www.small-journal.com

Table 1. Continued.

Mask's modification method	Active effect	Remarks of the modified mask	Ref.
Homogenous distribution of GNEC between two PP layer		1) Superhydrophobicity of the modified mask (CA 158°) 2) 100% bacterial filtration efficiency 3) Increasing the surface T of mask to >100 °C in 50 s in solar irradiation	[90]
Miscellaneous			
Coating the surface of compressed-polyure-thane face mask with TEOS then HDTMS	Hydrophobization	Increased the WCA from 85° to 133°.	[91]
Dip coating the whole nonwoven face mask into BAK	Biocidal effect of BAK	Preserve porous morphology of mask; 100% *phage ph 6* viral inhibition in 1 min	[92]
Developing new mask by nanofibrous membranes formation via electrospinning of PVA/licorice extract	Antiviral effect of licorice extract	Tuning the air permeability by adjusting the nanofiber diameters	[93]
Dip coating of the PP layer in a dispersion of QAC@h-BN NPs	Biocidal effect of QAC high heat conductivity of h-BN	Filtration efficiency (>99%) Enhance thermal conductivity of PP more than 7 times Kill 99% *E. coli* and 96% *S. aureus*	[94]
Incorporating of Cu/PAN-based filter mat to the mask structure	High heating production by Cu	1) Increasing the local temperature to 133 °C in 60 s in response to voltage 2 V 2) Ability to thermally kill the E. coli and SARS-CoV-2	[95]
Replacing the PP inner layer in multilayer masks with an electrospined PVA fibrous mat	TENG rule of PVA	1) Charge quantity of the medical mask 2) Rechargeability upon hand touching	[96]

Abbreviations: polypropylene (PP), polyacrylonitrile (PAN), water contact angle (WCA), polyamide 6.6 (PA66), influenza A virus (IAV), nanowires (NWs), reactive oxygen species (ROS), 2-diehtylaminoehtyl chloride (DEAE-Cl), graphene oxide (GO), triallyl isocyanurate (TAIC), polyvinylidene fluoride (PVDF), triboelectric nanogenerator (TENG), reduced graphene oxide (rGO), laser-induced graphene (LIG), graphene nanosheet embedded carbon (GNEC), tetraethyl orthosilicate (TEOS), hexadecyltrimeth-oxysilane (HDTMS), benzalkonium chloride (BAK), quaternary ammonium salts (QAC), boron nitride (h-BN), polyvinyl alcohol (PVA).

By taking advantage of Ag NPs, Kharaghani et al. prepared polyacrylonitrile/silver (PAN/AgNPs) nanofibers composite membranes by dipping the PAN nanofibers in AgNO$_3$ solutions for developing washable antibacterial masks.[75] The silver was highly stabilized on the surface of PAN fibers due to the formation of very stable complexes with the chelating aromatic heterocycles generated in the PAN chain backbone. These chelating agents are produced upon PAN pyrolysis which can further be catalyzed by the presence of Ag (**Figure 4**a).[112] This chelation increased the stability of the Ag NPs on the fabrics so that the fabrics could be washed without reducing their efficiencies. The SEM and TEM showed the uniform distribution of Ag NPs (20 nm in diameter) on the surface of PAN nanofibers (Figure 4b,c). Increasing the number of cycles of the dip coating increased the Ag content and therefore, increased the antibacterial activity of the fabrics by releasing more silver into the medium. However, very high contents of Ag NPs could lead to the generation of some aggregates with less antibacterial efficiencies. On the other hand, the leaching-out of Ag NPs has always been the challenge for such modification. Nevertheless,
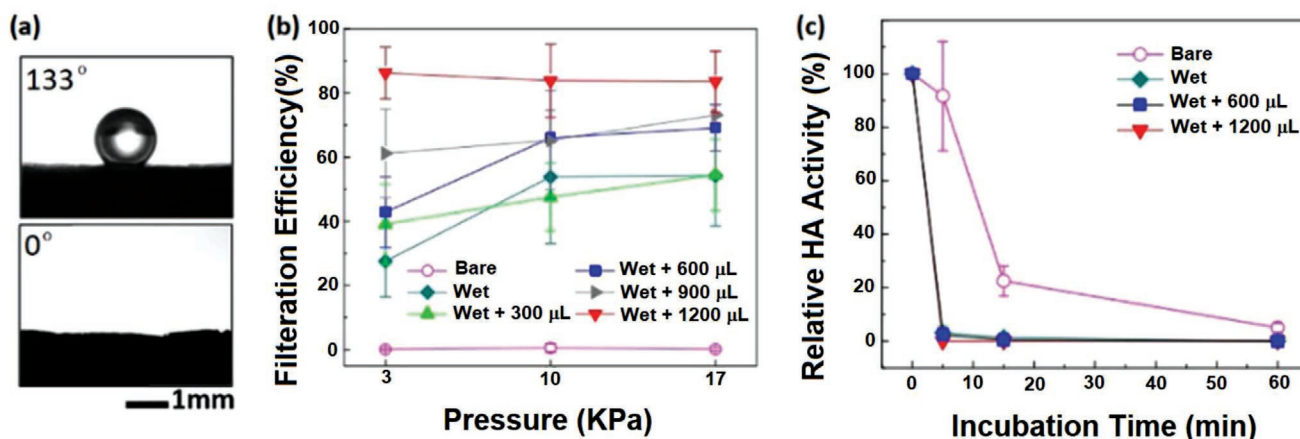

Figure 3. a) Comparison of the contact angle of bare PP (133°) with NaCl-coated PP (0°). b) Pressure-dependent filtration efficiency of salt-coated PP filters. c) Hemagglutinin activity (HA) of viruses adsorbed on salt-coated PP filters in various incubation times. Reproduced with permission.[71] Copyright 2017, Nature.
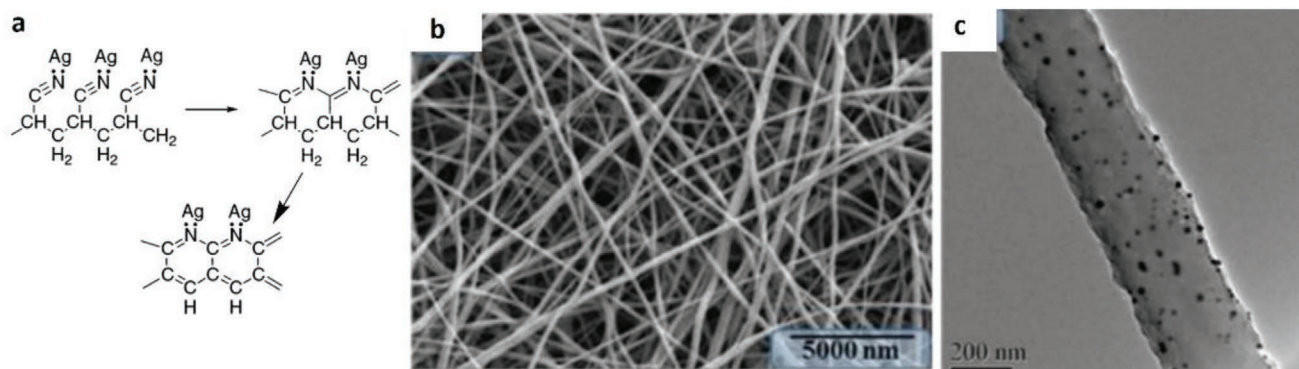
ADVANCED
SCIENCE NEWS
www.advancedsciencenews.com

NANO · MICRO
small
www.small-journal.com

Figure 4. a) Pyrolysis of PAN fibers in the presence of Ag, which leads to the generation of chelating agents in the PAN structure. Reproduced with permission.[112] Copyright 2003, American Chemical Society. b) SEM and c) TEM images of hybrid PAN/Ag nanofibers. Reproduced with permission.[75] Copyright 2018, MDPI.

this hybrid system showed effective antibacterial activity against *Pseudomonas* and *Staphylococcus* bacteria.

Hashmi et al. prepared CuO-loaded PAN nanofibers by electrospinning of a solution of PAN in DMF in the presence of dispersed CuO NPs and applied for the fabrication of antimicrobial breath masks.[76] The diameter of pure PAN nanofibers was around 141 nm which was increased to 161–197 nm by the addition of 0.25–1.0 wt% CuO NPs. The incorporated CuO NPs improved the mechanical strength of the nanofibers with negligible effect on the elongation at break. The CuO NPs also increased the air permeability of the nanofiber mats due to the increased porosity of dense PAN fibers caused by the NPs, thus facilitating the air flow among the fibers. The air permeability of nanofiber mats of PAN/CuO (1 wt%) were more than two times higher than that of nanofiber mats of pure PAN. The incorporated CuO NPs enhanced the hydrophilicity dramatically with water contact angle (WCA) of 124° for pristine PAN and zero degree for the PAN/CuO fibers. The incorporated CuO NPs could be slowly released from the nanofibers and generated strong antibacterial activity against *E. coli* and *B. subtilis*. However, high CuO content induced some toxicity in the masks. Indeed, NIH3T3 cell viability results showed the viability of around 88%, 78%, 75%, 68%, and 59% for nanofiber mats containing 0%, 0.25%, 0.5%, 0.75%, and 1.0 wt% CuO NPs. In another report, coating a hybrid nanocomposite layer of shellac/copper nanoparticles (CuNPs) on the surface of a nonwoven surgical mask using a microfluidic spray device affords a photoactive antiviral mask (PAM) with high hydrophobicity, self-cleaning, and reusable features (**Figure 5**a–d).[77] The simple process for this modification is depicted in Figure 5b. Shellac is a natural hydrophobic polyester with extensive application in bioadhesive and biocompatible coating materials;[113,114] while the nanosized copper particles are excellent antibacterial materials.[115] The SEM images (Figure 5e) clearly showed a homogenous coating on PP fibers by shellac/Cu nanocomposite layer. The WCA of the pristine nonwoven fabrics in the mask was around 111°, however, after 1 h the water droplet adsorbed into the fabric. By contrast, for the modified mask the WCA increased to 143° and the droplets did not adsorb onto the mask even after 1 h (Figure 5f). Shellac is also a well-known photoinitiator due to its adsorbing ability toward UV–vis light; and in parallel, CuNPs have robust interaction with light thanks to their surface

plasmon resonance excitation. Accordingly, solar illumination increased the surface temperature of the PAM mask to around 70 °C (Figure 5g) and therefore, could inactivate the SARS-CoV-2 facilely. Additionally, this process is reproducible, implying the reusability of the mask after simple self-cleaning and sterilization upon solar irradiation. Also, the coating by the nanocomposite layer showed a negligible effect on the filtration efficiency of the mask. The modified photoactive mask showed strong antibacterial activity (>99.99% for *E. coli*) upon solar irradiation.

Gopal et al. proposed the application of Zn-embedded polyamide 6.6 (PA66) for the fabrication of face masks with the ability to capture and then inactivate SARS-CoV-2 and influenza A virus (IAV) H1N1.[78] Comparison of the amounts of the virus captured by cotton, PP and PA66 after impregnation in the virus medium showed that liquid retention and virus retention on PP has the lowest amount due to its hydrophobicity. On contrary, the retention on cotton and PA66 was higher due to the hydrophilicity of these fabrics. However, washing the textiles with tween-80 (without inactivating the virus) showed that around 90% and 60% of the virus could be removed from the PA66 and cotton, respectively. This clearly indicated the higher washability of PA66 than cotton for the remaining antiviral effect. Since Zn(II) salts can inactivate viruses,[116] after capturing the viruses by PA66 mask, viral deactivation can be induced by Zn(II). One of the significant advantages of Zn(II) over Cu(II) is the less toxicity of Zn(II) against normal cells. Incubation of the PA66 fabrics bearing Zn(II) ions with IAV and SARS-CoV-2 led to around 2-log of reduction of viruses in titer tests for 1 h.

Kumar et al. tried to combine the advantages of both Zn(II) and Cu(II) and incorporate them simultaneously into the PP-based MERV15 filter material (three-layer) to provide reusable antimicrobial masks.[79] Specifically, thin copper@ZIF-8 core–shell nanowires (Cu@ZIF-8 NWs) with average diameter 80 nm (**Figure 6**a,b) were fabricated using biocompatible pluronic F-127 copolymer as a stabilizing agent and adhered to the PP layer of face mask (Figure 6c).[79] Immobilization of the Cu@ZIF-8 NWs onto the PP layer was performed by simple dip-coating of the PP layer in dispersions of NWs in ethanol. This modification did not change the hydrophobic character of PP. However, it improved the filtration efficiency of the mask (Figure 6d). On contrary, treating PP with pure ethanol declined the filtration efficiency dramatically, which was probably due to the loss of
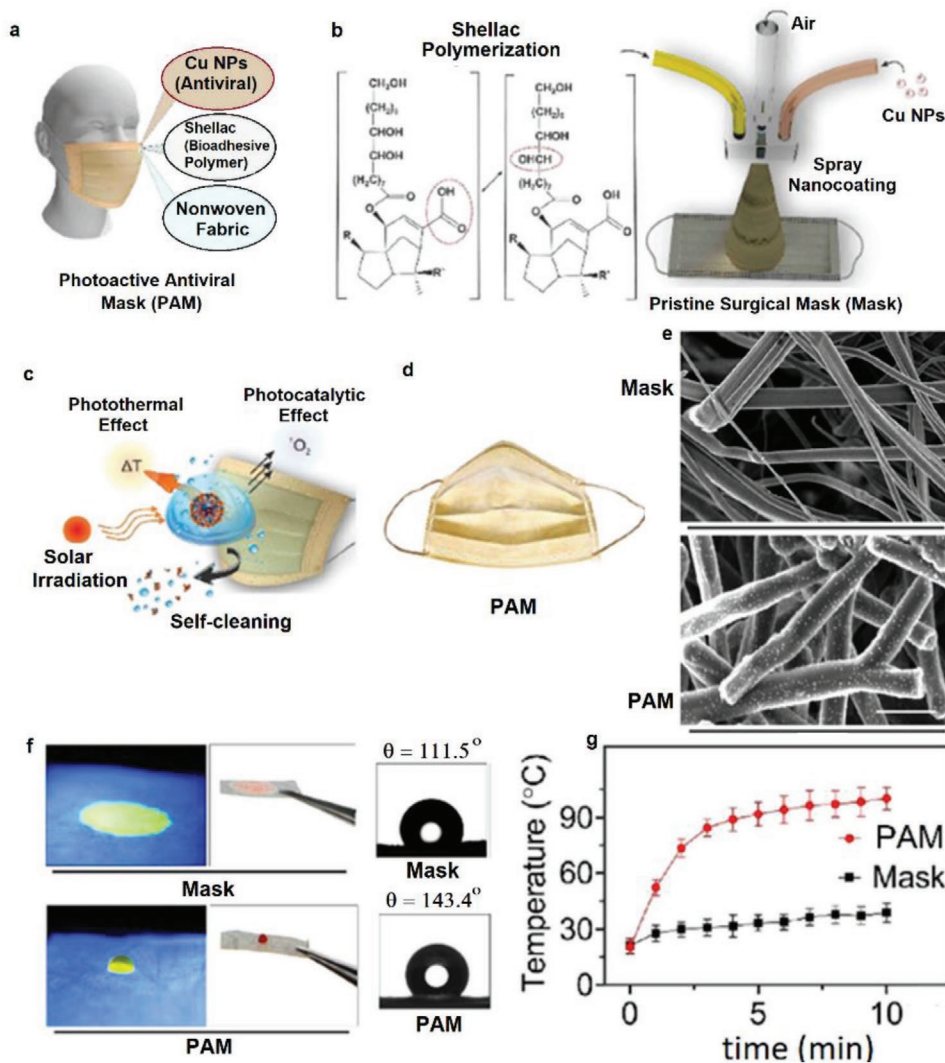
ADVANCED
SCIENCE NEWS
www.advancedsciencenews.com

NANO · MICRO
small
www.small-journal.com

Figure 5. a) General representation of the components of the nanocomposite layer on the surgical mask. b) Schematic illustration for the spray coating of the shellac/Cu nanocomposite layer on the surface of the nonwoven PP fibers using a microfluidic device. c) Virus inactivation by various photothermal and photocatalytic mechanisms upon solar irradiation and self-cleaning due to the hydrophobicity of the modified surface. d) The appearance of the modified photoactive antiviral mask (PAM). e) SEM images of the nonwoven PP fibers before and after coating with shellac/Cu nanocomposites. f) Contact angle and water-adsorption behavior of the masks. g) Increasing the temperature of the pristine and modified mask upon solar irradiation versus time. Reproduced with permission.[77] Copyright 2021, American Chemical Society.

surface charges of the PP layer, as reported by others as well.[117] Coating the Cu NWs with a ZIF layer improved the biocompatibility and reduce the cytotoxicity of copper due to the slower release rate of Cu ions. Additionally, the antibacterial activity of hybrid Cu@ZIF-8 NWs was much stronger than that of Cu NWs or ZIF-8 alone against *E. coli* and S. *mutans* (Figure 6e). The reason was related to the slow degradation of the NWs and co-release of Zn(II) and Cu(II) ions which can kill the bacteria. Furthermore, the antiviral activity against SARS-CoV-2 using virus-infected Vero E6 cells showed around 55% inhibition of virus replication in 48 h with cell viability of 99% (Figure 6f,g).

In summary, the incorporation of selected metal-based NPs and water-soluble salts can endow the masks with high antimicrobial activity. However, there are some challenges that need to take into consideration for practical applications. i) The water-soluble salts can easily be washed away from the mask and thereby the efficiency of the mask reduce dramatically. ii) Leaching out of metal NPs can endow allergy or other side effects on the human body. Therefore, a wide-range evaluation of the toxicity of the active components embedded in the masks is essential. Additionally, there are some other types of antimicrobial metal-based NPs reported, such as Fe,[118] Au,[119] Mg,[120] and the feasibility of those NPs for rendering the masks antimicrobial and antiviral should be investigated. Moreover, it is worthwhile identifying proper carriers for metal NP, like micro- or mesoporous materials, to minimize the leaching effect.

4.2. Photosensitizers

Photosensitizers are groups of organic/inorganic compounds that can capture the energy of the light and transfer it to the
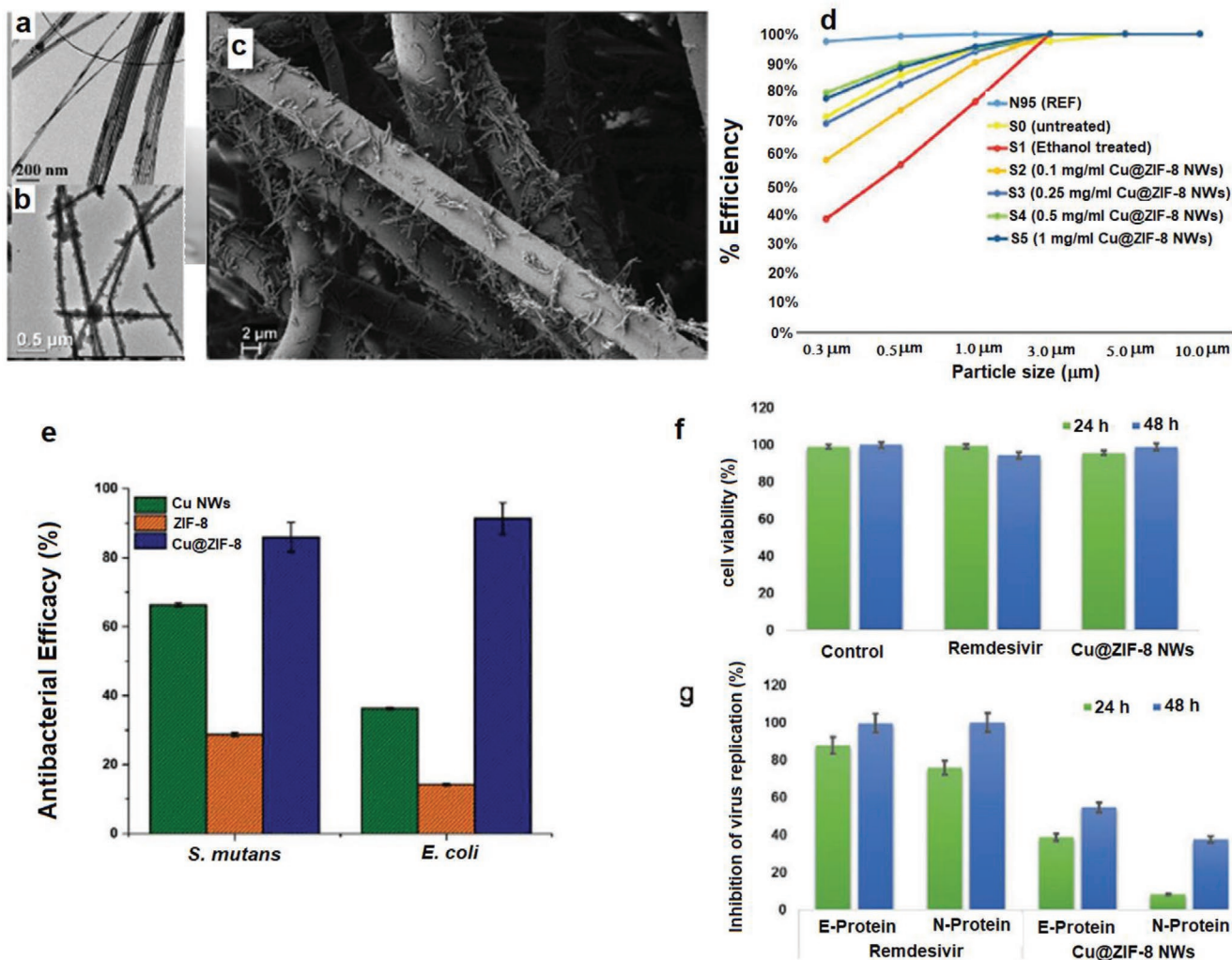
Figure 6. TEM images of a) Cu NWs and b) Cu@ZIF-8 NWs. c) SEM image of fibers of face mask coated by dip coating in 1 mg mL^{-1} dispersion of Cu@ZIF-8 NWs. d) Filtration efficiency of the face masks before and after functionalization with Cu@ZIF-8 NW. e) The antibacterial performance of Cu NWs, ZIF-8, and Cu@ZIF-8 NWs. f) Toxicity of Cu@ZIF-8 NWs and Remdesivir against Vero E6 cells, and g) antiviral efficiency of Cu@ZIF-8 NWs and Remdesivir at 24 and 48 h postinfection. Reproduced with permission.[79] Copyright 2020, Wiley.

surrounding oxygen to generate extremely reactive oxygen species (ROS).[121,122] The produced ROS can kill all microorganisms in a short time.[123] Therefore, ROS-generating materials have been incorporated into textiles and fabrics for improving the antimicrobial properties of these materials. For instance, conjugation of 3,3′,4,4′-benzophenone tetracarboxylic acid photosensitizer to cotton fabrics enabled 99.99% inhibition of *E. coli* and *S. aureus* under UV light exposure.[124] Similarly, grafting of photoactive anthraquinone-2-carboxylic acid onto the silk fibroin/cellulose acetate blend nanofibrous membranes showed 99.9999% contact-killing of *E. coli* under UVA irradiation.[125]

There are several reports about the incorporation of ROS generators in the face masks to capture and inactivate the bacteria and viruses during breathing, thereby preventing lung infection. Monge et al. also incorporated the photoactive conjugated polymers and oligomers into the masks and other PPEs as strong materials for the inactivation of SARS-CoV-2.[80] Accordingly, three oligomeric phenylene ethynylenes and two conjugated polymers (see **Figure 7**) were examined. By incubation

of oligomers and polymers with SARS-CoV-2 and exposing the medium to near UV (300–400 nm) or vis (420 nm) light, the infection of SARS-CoV-2 on Vero cells was reduced quickly and effectively (Figure 7). Hydrophobic and electrostatic interactions between ionic conjugated polymers and oligomers with SARS-CoV-2 spike protein were the main reason for antiviral activities. Indeed, these interactions bind the virus to the material which then upon light irradiation generates ROS, leading to the rapid degradation of the virus. Oligomers 1 and 3 and polymer 5 showed the most powerful antiviral activity with complete inhibition in ≈20, 10, and 60 min, respectively. It is worth mentioning here that despite the strong inherent antibacterial activity of polymeric quaternary ammonium 4[126] it showed no activity against SARS-CoV-2 on dark condition. Therefore, using conventional quaternary antibacterial materials for deactivating SARS-CoV-2 is unlikely appropriate.

Tang et al. immobilized the anionic photosensitizers onto the cationic cotton cloth to fabricate a daylight-induced antibacterial and antiviral cloth as a face mask.[81] The cationic cotton
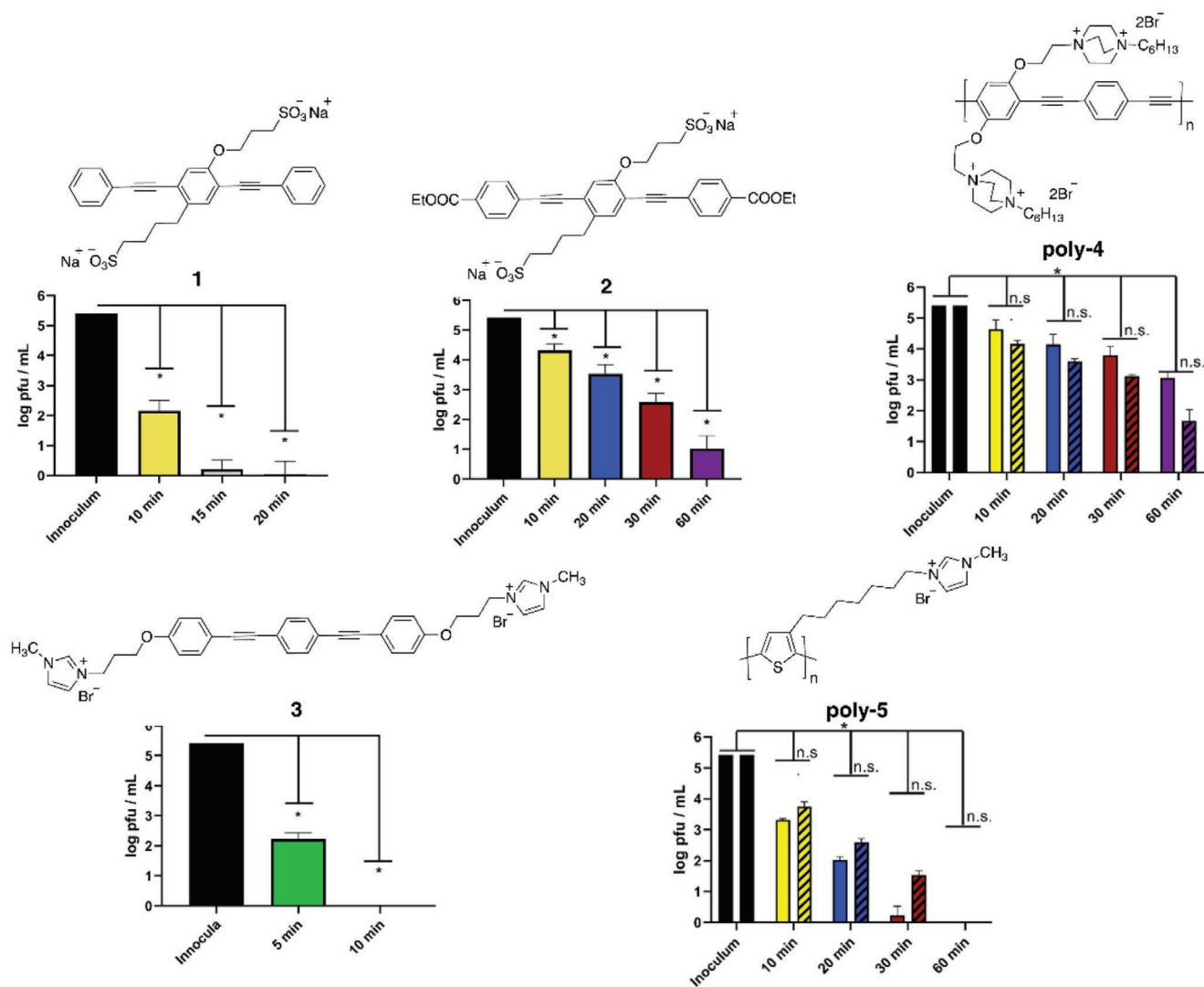
Figure 7. Structures of photoactive conjugated polymers and oligomers and their corresponding antiviral activities against SARS-CoV-2 upon near-UV light irradiation at various times. Reproduced with permission.[80] Copyright 2021, American Chemical Society.

fabrics were prepared by surface grafting of cotton fabrics with 2-diehtylaminoehtyl chloride (DEAE-Cl) in alkaline condition. The resulting cationic fabric was postfunctionalized via electrostatic interactions with anionic photosensitizers (**Figure 8**a) which can release ROS under light exposure. Functionalization of cotton fabrics by polyDEAE along with photosensitizers (Rose Bengal, RB & sodium 2-anthraquinone, 2-AQS), without having any impact on the morphology of the fabrics (Figure 8b–e), improved the antibacterial efficiency dramatically. While pristine cotton fabrics showed no biocidal activity, the inhibition rate against *E. coli* and *L. innocua* for cotton@polyDEAE were around 98% and 86%, respectively, in 30 min; and further increased to >99.99% (under light exposure) for both bacteria after incorporation of photosensitizers. However, the biocidal activity was severely reduced to almost 0% in dark condition. Furthermore, the antiviral evaluation against T7 bacteriophage (a model virus with even higher ROS resistance than coronavirus) showed no activity for pristine cotton and cotton@polyDEAE whereas the photosensitizers-bearing

fabrics showed strong ability in inactivating T7 bacteriophage (Figure 8g). Importantly, the modified fabrics were washable and after three times washing and 7 days exposing to light only negligible reduction in the biocidal performance was observed. The findings from the work above demonstrated that simply cationic modification of fabrics, via grafting quaternary ammonium groups, is not sufficient to render the fabric antiviral. Further modification of such conventional disinfectant is essential for enhancing the performance.

TiO$_2$ is well-known for its photoactive properties via releasing ROS upon UV irradiation[127,128] with a strong ability to inactivate various viruses including SARS-CoV-2 as reported very recently.[129,130] Horváth et al. prepared photocatalytic TiO$_2$ nanowires (TiO$_2$NWs)-based filters for the construction of cost-effective and reusable masks with antimicrobial properties (**Figure 9**).[82] TiO$_2$NWs have high processability and can produce freestanding and flexible films (Figure 9c) without leaching nanowires under normal flow conditions.[131] The obtained textile showed strong antibacterial activity against
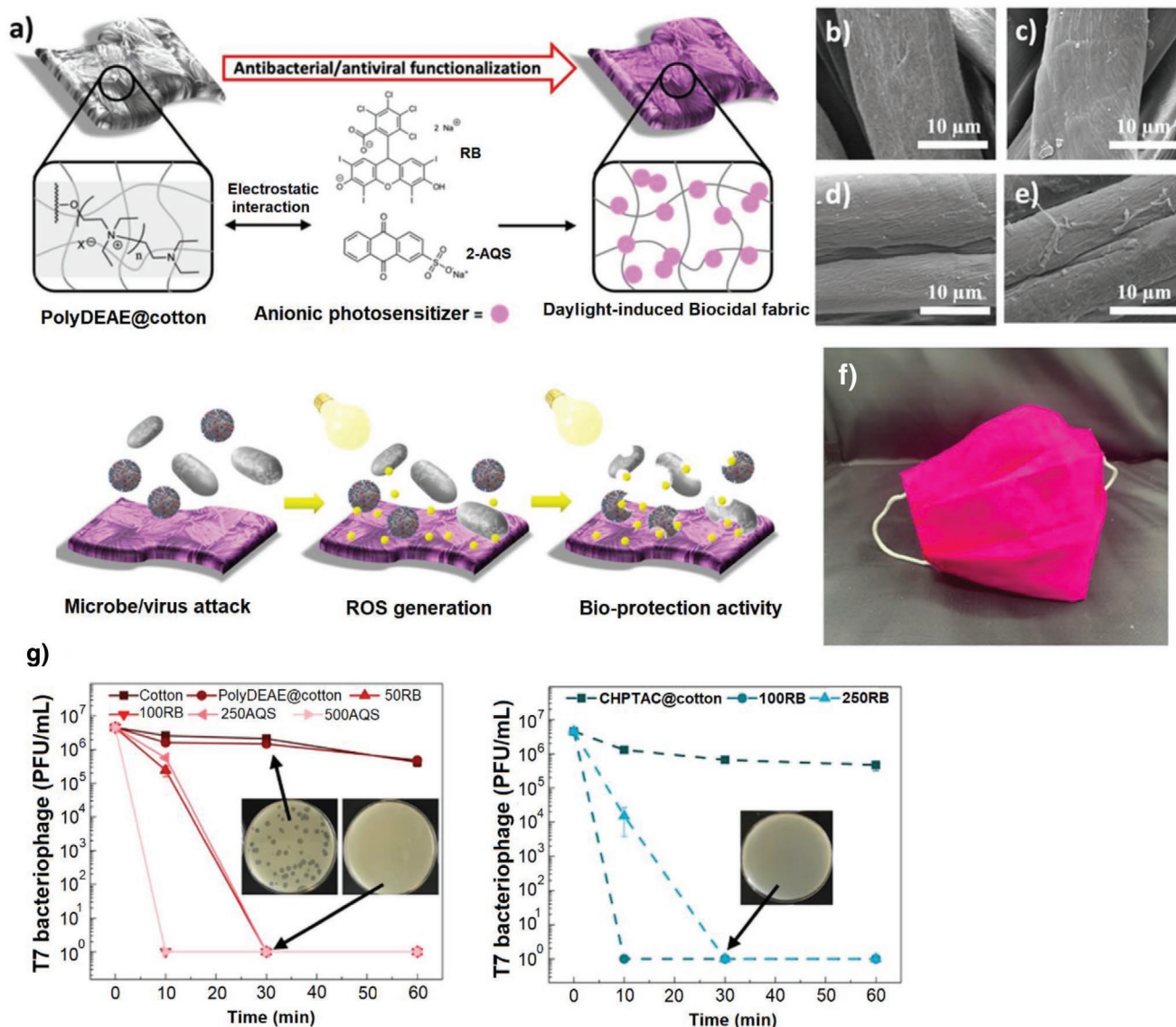
ADVANCED
SCIENCE NEWS
www.advancedsciencenews.com

NANO · MICRO
small
www.small-journal.com

Figure 8. a) General description for the preparation of the daylight-induced antimicrobial cotton cloth (below show the daylight-induced ROS generation and thereby inhibition of microorganisms). SEM images of b) pristine cotton, c) polyDEAE@cotton, d) RB@polyDEAE@cotton, and e) 2AQS@ polyDEAE@cotton. f) Fabrication of facemask using the obtained photoactive cotton textiles. g) Antiviral efficiency of photoactive fabrics under daylight irradiation at various times. Reproduced with permission.[81] Copyright 2020, American Chemical Society.

E. coli under UV light (365 nm) and almost all the bacteria were inactivated in 1 min whereas the control using Teflon filter under the same UV irradiation showed weak antibacterial properties (Figure 9d). This textile could be applied for the fabrication of light sterilizable face masks (Figure 9e,f) with the ability to reuse more than 1000 times.

Overall, while photosensitizers are shown to be effective agents for endowing the masks with antimicrobial and self-sterilizing properties, they lose their efficacies in the absence of light. Therefore, in cloudy weather, during the daytime with less sun illumination, and in the areas with less sun irradiation, the effectiveness of the masks containing photosensitizers will be lowered substantially or even lost completely at extreme conditions. Therefore, incorporating compounds such as

endoperoxides[132] and phenalenone-based photosensitizers[133] that can release ROS even under dark conditions can be considered as a proper solution to tackle this problem. On the other hand, the results on the antiviral performance of those photosensitizers are rather limited. Particular attention should be paid to the antiviral activities against coronavirus in future research.

4.3. Graphenes

Graphene-based materials have been used extensively in biomedical applications.[134–136] Especially after the outbreak of the SARS-CoV-2 pandemic there have many reports on utilizing graphene-based materials for fighting against this virus,[137–139]
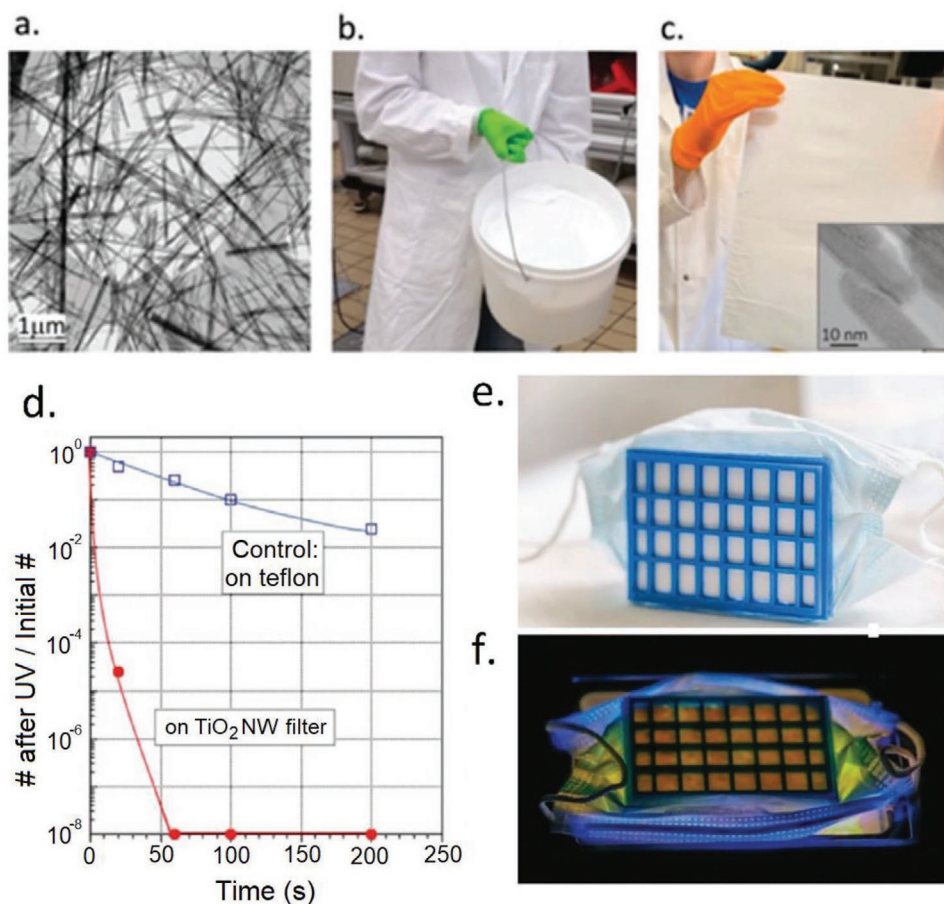
Figure 9. a) SEM image titanate nanowires as the precursors for TiO$_2$ NWs. b) The scale up production of titanate nanowires. c) A fabricated filter paper from TiO$_2$ NWs after spreading of titanate nanowires and calcination thermal treatment. d) Comparison of the bacterial inhibition performance of TiO$_2$NWs filter with the control Teflon filter. e) Construction of a mask prototype by connecting the TiO$_2$NWs filter paper to a 3D-printed plastic frame. f) Decontamination of the mask by UV irradiation. Reproduced with permission.[82] Copyright 2020, Wiley.

including some related to the use of graphenes in face masks. The key and unique properties that graphenes can endow in the masks include i) superhydrophobicity of graphenes increases the wetting resistance of the mask by aerosols containing viruses and bacteria and enhances the self-cleaning of the masks, ii) excellent electrothermal behavior of graphenes can create local high temperatures which can easily inactivate the microorganisms, and iii) inherent antimicrobial properties of the graphene-based nanomaterials.

Inserting the graphenes into the mask structures is often performed via the following strategies. i) Fabrication of some paste or inks of graphenes, which are then spread on the layer of mask. The properties of the layer can be tuned by adjusting the composition of the paste/ink mixture. The addition of other components to the paste has been attempted to create hybrid materials. ii) In situ generation of graphenes on the surface of masks by well-established techniques such as laser-induced forward transfer (LIFT).

Zhao et al. immobilized graphene oxide (GO) onto the cotton fabrics by three different methods to render the fabrics antibacterial and antiviral for fabrication of face masks.[83,84] The 1st method involves the filtration of aqueous GO suspension through the cotton fabrics. Therefore, GO particles are adhered to the fabrics by strong van der Waals and H-bonding interactions. For the other two methods, the fabrics were first soaked in an ethanol solution of triallyl isocyanurate (TAIC, a radical crosslinker) and then applied for the filtration of GO suspension. Subsequent crosslinking polymerization of TAIC by γ-irradiation (the 2nd method) or thermal polymerization (3rd method) improved the stability of GO on the fabrics. All the GO-modified fabrics showed antibacterial inhibitions >99% against *E. coli* and *B. subtilis*. However, washing the fabrics removed the GO from the fabric made by the 3rd method; whereas the GO remained adhered to fabrics over the 1st and 2nd methods. Indeed, the incorporation of low polar TAIC reduces the interaction between GO with fabrics. However, γ-irradiation can generate radicals on all components including GO and cotton by breaking the σ linkages. The coupling of generated radicals can stabilize the GO on the surface of fabrics. Furthermore, the animal tests showed no irritation to rabbit skin after 3 days.[83] Later, evaluation of the antiviral efficiencies showed nearly complete inhibition against SARS-CoV-2 viral.[84]

The N95 masks are multilayers in which the middle layer of PP, prepared usually via melt-blown extrusion, has electrostatic charges that attract the viruses and help to improve the filtration efficiencies over 95%. However, these electrostatic charges
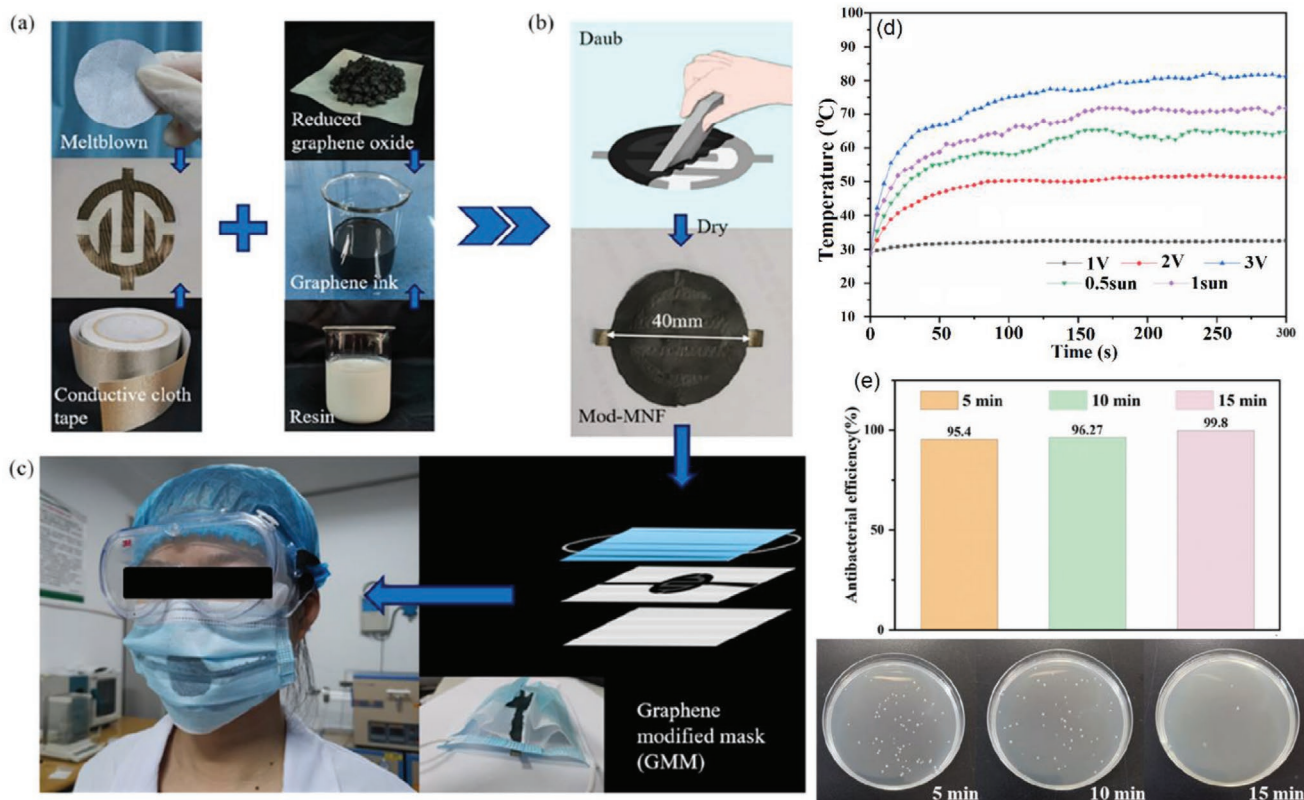
Figure 10. a–c) Schematic description for the fabrication of electrothermal graphene-modified masks. d) The temperature of the graphene-modified MNF in response to different voltages. e) Antibacterial activity of graphene-modified MNF against *E. coli* under different electrifying times. Reproduced with permission.[86] Copyright 2020, American Chemical Society.

often disappear after around 8 h exposure to the environmental conditions,[140] which, therefore, reduce the efficiencies of N95 masks remarkably. Incorporation of hydrophobic TENGs into the membranes, films, and fabrics have been proposed as a reliable method for increasing the lifetime of the electrostatic charges. For instance, Lv et al. prepared a single-electrode TENG using a hydrophobic ionic liquid gel which was stable under different environmental conditions for 3 months with humidity up to 80%.[141] Figerez et al. embedded the GO NPs in the friction layers of masks which acted as a TENG with high electrostatic charge retention capacity and excellent recharge-ability even at humid medium.[85] Specifically, the PP layer in the N95 mask was simply coated by an ink paste composed of polyvinylidene fluoride (PVDF) and GO in isopropanol to improve the triboelectric voltage and charge of the PP layer.[85] The high hydrophobicity of PVDF in the casting ink increased the WCA from 103° for pristine PP to 133° for the modified PP. Applying the pressure with the thumb pressing generated the voltages of around 7 and 17 V and the charges of 1.5 and 2.0 nC cm^{-2} on the pristine and modified PP monolayers, respectively, with the charge retention periods up to 2 and 5 days. The modified PP layer was sandwiched between cotton and nylon fabrics to assemble a three-layer N95 mask. This trilayer mask can be readily recharged by simple mechanical movements such as hand-bending or sliding one over the other. Accordingly, the effective lifetime of the N95 mask by this strategy could be enhanced significantly. In another report,

graphene was used as a local heat generator for disinfection to provide reusable self-sterilization masks.[86] The simple process of fabricating electrothermal graphene filters and embedding them into the mask structure is depicted in **Figure 10**a–c. In the first step, a patterned flexible conductive cloth tape, as inter-digital electrodes, was attached to the surface of a filter layer composed of melt-blown nonwoven fabrics (MNF). Then, the graphene-modified MNF (mod-MNF) was produced by coating a graphene layer (graphene ink = reduced GO + silicone modi-fied acrylic resin + amino resin + polyvinylpyrrolidone + water) with high electrical and thermal conductivity onto the MNF. The electrothermal/photothermal behavior of the mod-MNF is depicted in Figure 10d. By increasing the applied voltage to the electrodes, the temperature was raised to 80 °C at 3 V in 4 min. Also, irradiation by the simulated sunlight increased the temperature to around 72 °C. The elevated temperature could kill the *E. coli* bacterium with the efficiencies of 95% and 99.8% by electrifying for 5 and 15 min, respectively, indicating strong self-sterilization (Figure 10e). Furthermore, the graphene-modi-fied masks showed the air permeability and filtration efficiency similar to the unmodified masks. The performance of the mask remained unchanged after folding/unfolding 200 times, implying the high durability of the masks.

Using laser to convert and pattern carbon precursors (e.g., polyimide, SPEEK, and Bakelite) directly into graphene (called laser-induced graphene, LIG) has proved as a scalable and cost-effective method for fabricating functional graphene.[142]
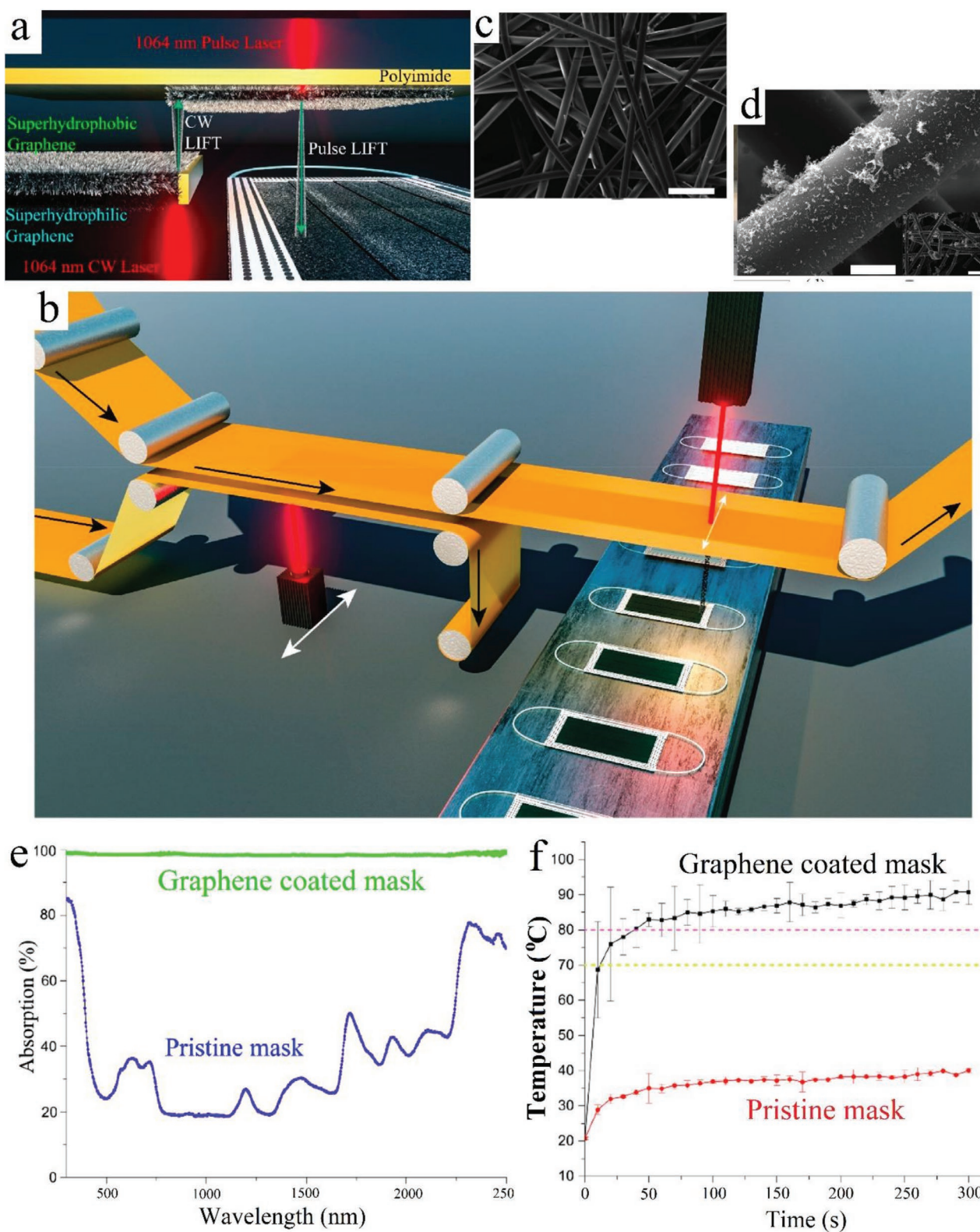
Figure 11. a) The fourth-generation dual-mode LIFT to continues-LIFT transfer of graphene onto a second polyimide followed by a then pulse-LIFT transfer of graphene onto the mask surface. b) Description for the simple scale up of this strategy via roll-to-roll production of a graphene-coated mask. SEM image of c) pristine nonwoven fibers and d) graphene-coated nonwoven fibers. e) Optical absorption behavior of pristine and graphene-coated masks. f) The temperature of the surface of pristine and graphene-coated masks in response to solar illumination. Reproduced with permission.[87] Copyright 2020, American Chemical Society.

ADVANCED
SCIENCE NEWS
www.advancedsciencenews.com

NANO · MICRO
small
www.small-journal.com

By adjusting the processing conditions, a superhydrophobic graphene can be obtained.[143] Additionally, the LIFT graphene has a strong photothermal activity which makes it a powerful antibacterial agent.[144] Accordingly, a dual-mode LIFT process was reported by Zhong et al. for tethering a graphene layer on the surface of commercial surgical masks to provide superhydrophobic and photothermal porous layers.[87] The schematic process for the modification is presented in **Figure 11**a,b. The SEM images (Figure 11c,d) clearly showed the smooth microfibers for the pristine mask and the appearance of nanostructured flakes attached to the microfibers. The modified mask with a black appearance was superhydrophobic (CA 140°) so that the water droplet could move freely on the graphene-coated surfaces of mask without wetting the mask surface. Study on the photothermal performance of the mask showed that the pristine mask weakly absorbed the solar spectrum whereas the graphene-coated masks adsorbed over 95% of the solar spectrum in the range of 300–2500 nm (Figure 11e). Accordingly, the solar light irradiation of the masks increased the temperature of the pristine mask to 45 °C in 5 min whereas the temperature of the modified one was increased to 70 °C in 50 s and further increased to 80 °C after 100 s (Figure 11f).

In the extension of the previous work, Zhong et al. deposited Ag NPs along with graphene onto N95 masks by LIFT strategy to provide a plasmonic photothermal and superhydrophobic layer on the mask with highly improved antimicrobial protection.[88] The methods for this immobilization are depicted in **Figure 12**a,b. The first method (M1) involves the deposing of only Ag NPs whereas in the second method (M2) a layer of Ag NPs and graphene are simultaneously deposited on the N95 surface. Ag NPs create the plasmonic effect and antimicrobial effect whereas the incorporated graphene further improves the photothermal property and hydrophobicity of the modified mask. The plasmonic effects of M1 and M2 (Figure 12c) were much higher than pristine surfaces. Also, the WCA (Figure 12d) showed that neat Ag NPs increased the hydrophilicity (68°) whereas co-immobilization with graphene endows strong hydrophobicity to the surface (140°). Visible light irradiation showed that after 5 min the temperature of the surface of pristine and M1 increased slightly to less than 40 °C whereas for M2 temperature increased to 60 °C in 10 s and further reached to 80 °C in 1 min (Figure 12e). Both elevated temperature and superhydrophobicity are foreseen to inactivate the SARS-CoV-2[145] but specific results on antiviral activity were not reported in the work addressed above.

In another strategy, the laser-inducing technique was used for converting a polyimide (PI) film (thickness 0.05 mm) directly to porous graphene or LIG.[89] Principally this technique can be applied to fabricate porous graphene from various types of other commercial polymers and is not limited to PI.[146] Lasing PI in an inert atmosphere yielded a hydrophobic LIG with WCA 150° whereas lasing in an ambient atmosphere afforded a hydrophilic LIG with WCA 20°. Antibacterial experiments showed that for the commercial masks based on activated carbon fiber (ACF) and melt-blown fabrics (MBF), more than 90% of *E. coli* deposited on mask surface remained alive after 8 h. On the other hand, the bacterial inhibition of pristine hydrophobic LIG was around 82% which was increased to 99.998% after solar irradiation for 10 min. Upon sunlight illumination,

the surface temperatures of MBF, ACF, and LIG were increased from 25 to 35, 52, and 62 °C, respectively, after 1 min. While no antiviral study was performed using LIG mask, however, high temperature generated upon solar irradiation has been proved promising for inactivating the SARS-CoV-2 virus.[89]

Moreover, a nanolayer of graphene nanosheet embedded carbon (GNEC) film was uniformly distributed on the melt-blown PP fibers to generate a superhydrophobic, photosterilizable, and reusable mask.[90] The general process for the fabrication of GNEC and embedding in the mask composition is depicted in **Figure 13**a,b. The GNEC was produced first on the Si substrate using electron cyclotron resonance sputtering system (Figure 13a) and then distributed uniformly between the melt-blown fibers with the aid of ultrasonic extrusion after exfoliating from the Si surface. The WCA for the pristine mask and GNEC mask were around 113° and 158°, respectively. This superhydrophobic character inhibits the adsorption of the respiratory droplets bearing virus and bacteria to the surface of the mask. Furthermore, the filtration efficiency of the GNEC mask was improved significantly due to the blockage of some large holes in the pristine mask after embedding with GNEC. Indeed, the values for bacterial filtration efficiency (d 2.5 µm) and particulate filtration efficiency (d 0.3 µm) were increased, respectively, from 95% and 35%, for pristine mask to 100% and 94% for GNEC mask. The solar illumination of the mask increased temperature to 105 °C in 50 s, which is sufficient to inactive most of the viruses (Figure 13c).

4.4. Miscellaneous Other Methods

Several other methods have also been explored or adopted by researchers for endowing some especial properties in the mask structure such as coating the surface of the mask with alkylsilane groups to improve the hydrophobicity of the polyurethane masks,[91] by biocide agents to increase the antimicrobial activity,[92,93] or by boron nitride[94] and copper metal[95] as excellent thermal conductive materials.

Ray et al. improved the hydrophobicity of the masks by coating a monolayer of highly hydrophobic hexadecyltrimethoxysilane (HDTMS) on the surface of masks.[91] The face mask made from compressed-polyurethane typically has a microporous structure with the ability to block 99% of the particles of pollen size and can be reused easily after washing. However, its high hydrophilicity reduces its efficiency significantly after it becomes wet. To address this problem, the hydrophobization of its surface was conducted via a two-step silylation, i.e., first by the hydrolysis of tetraethyl orthosilicate (TEOS) on its surface, followed by coating with a monolayer of HDTMS.[91] The WCA of the pristine mask was 85° which, however, became zero after 15 min when the water droplet was completely absorbed by the mask. On the other hand, the WCA for the modified mask was increased to 132° which remained unchanged after 15 min, indicating stable hydrophobicity of the surface. Soaking the modified mask in water and squeezing the mask samples showed almost no decrease in the Si content indicating the strong connection of the Si layer to the mask surface with guarantee its reusability after washing. Martí et al. modified the surface of nonwoven face mask filter
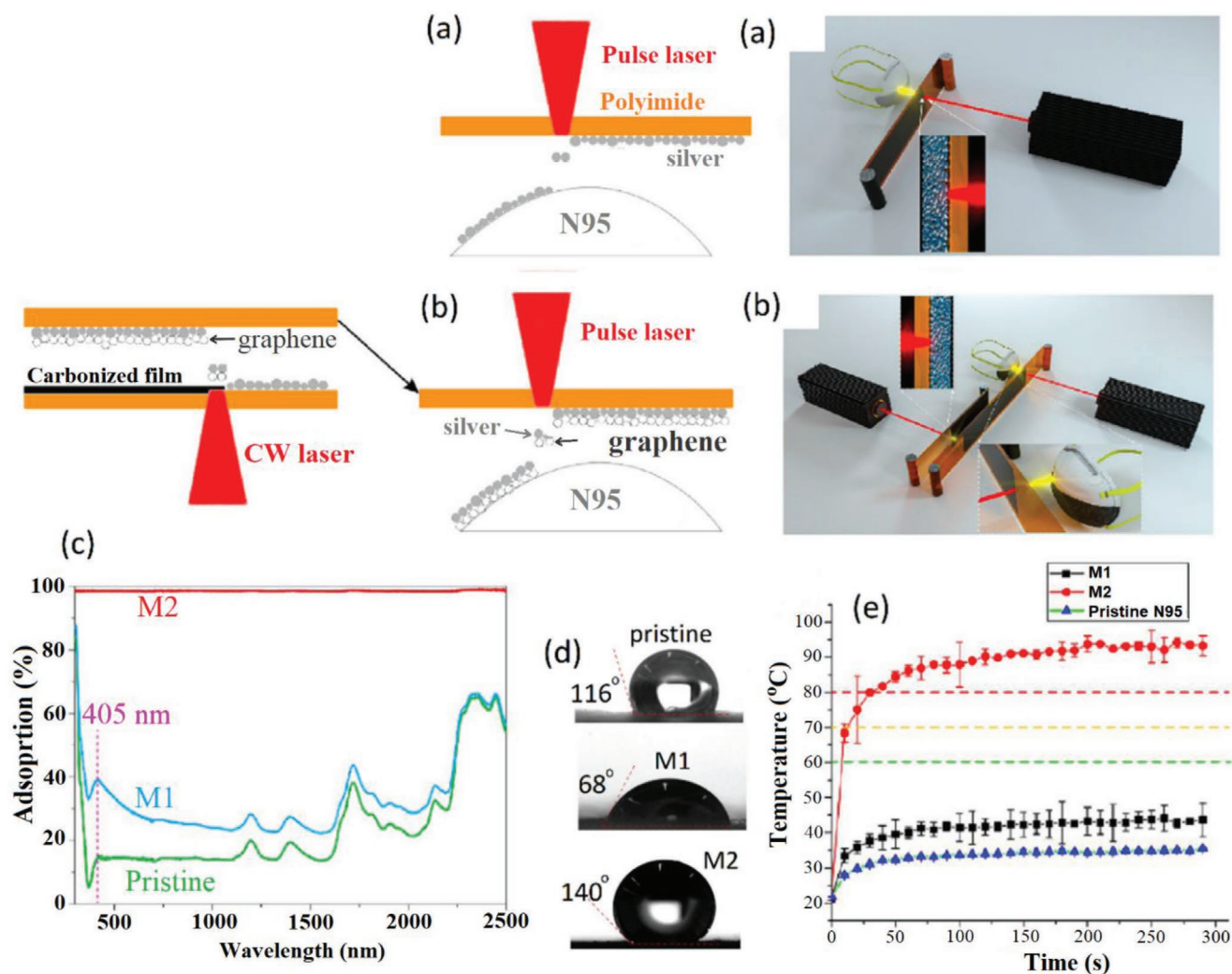
Figure 12. a) M1 laser printing procedure for the coating of neat Ag NPs on the N95 mask surface. b) M2 two-step laser printing procedure for co-immobilization of Ag and graphene on the N95 mask surface. c) The optical absorption behavior of pristine, Ag-coated (M1) and Ag/graphene-coated (M2) N95 mask. d) Contact angle of pristine and modified masks. e) Photothermal behavior of pristine and modified masks under sun irradiation. Reproduced with permission.[88] Copyright 2020, American Chemical Society.

by dip coating in an ethanol solution of 0.1% benzalkonium chloride (BAK) to create antibacterial property in the mask surface along with capability for the inactivation of SARS-CoV-2.[92] This coating did not induce a detrimental effect on the porous morphology of the fibrous nonwoven mask. Also, the modified mask showed strong antiviral activity with almost 100% viral inhibition in 1 min against *phage ph 6* (a viral model of SARS-CoV-2). On the other hand, the untreated mask and the mask treated only with ethanol showed no antiviral activity. Furthermore, the BAK-modified mask showed strong inhibition activity against methicillin-resistant *S. aureus* (MRSA) and *S. epidermidis* (MRSE) bacteria. Despite this strategy appears to be facile, without the results on biocompatibility, it is still doubtful whether this modified mask is feasible for practical applications since the BAK can be readily leached out of the surface of the mask by moisture, potentially leading to skin and lung contamination upon contacting with face and breathing.

In another safer approach, the extracts of licorice roots as bio-based antiviral agents were embedded into the mask structure,[93] while the extracts already demonstrated powerful antiviral activities against various viruses including RSV, HIV, and SARS-CoV.[147,148] Practically, electrospinning of an aqueous solution of polyvinyl alcohol (PVA) containing licorice roots extracts was used to prepare nanofibrous membrane as the active layers of the mask (**Figure 14**a). Air permeability and breathability of the masks could easily be controlled by tuning the size of the nanofibers (Figure 14b). Although this method appears to be very safe and effective for the fabrication of bio-based antiviral masks, no antimicrobial studies were reported by the authors.

The weak heat diffusion efficiency of the PP layer in masks creates an unpleasant sweltering sense while wearing. Accordingly, Xiong et al. developed hexagonal boron nitride(h-BN)/PP nanocomposite fibrous membranes to fabricate face masks with high comfortability and antibacterial activity.[94] The fabrication
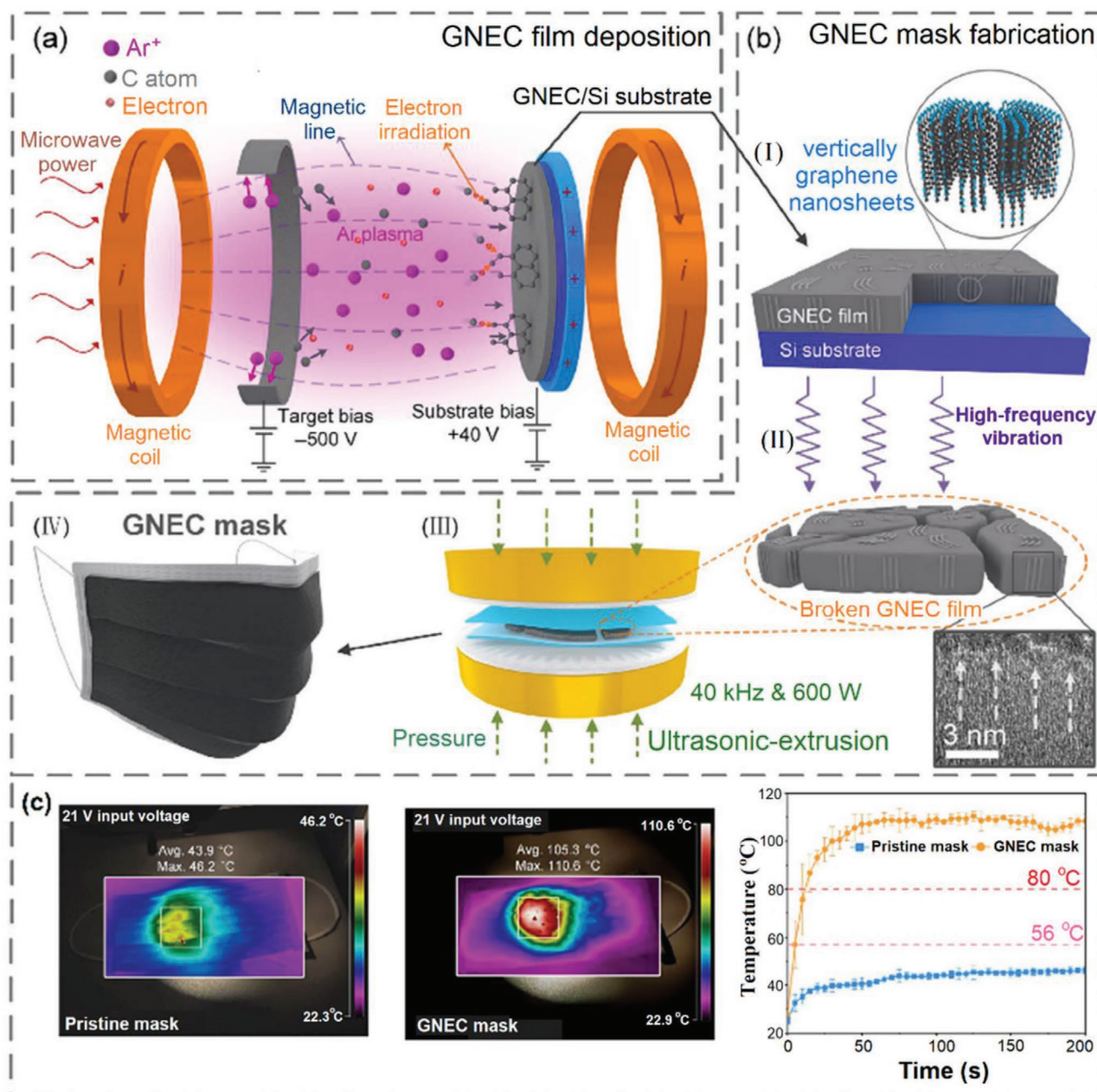
Figure 13. a) Immobilization GNEC film on the Si substrate using cyclotron resonance (ECR) sputtering system. b) Embedding of the GNEC into the mask structure i) vertically deposited graphene nanosheets with thickness 70 nm, ii) exfoliating the GNEC film with high-frequency vibration, iii) ultrasonic-extrusion (40 kHz and 600 W) for homogeneous distribution of GNEC thin layer between the melt-blown fibers, and iv) the fabricated GNEC mask. c) Photothermal activity of pristine and GNEC mask for 200 s solar irradiation. Reproduced with permission.[90] Copyright 2020, Springer.

included i) plasmas bombardment of h-BN NPs to create OH groups on the NPs' surface followed by functionalization with quaternary ammonium salts (QAC) through reaction with 3-(trimethoxysilyl)-propyl dimethyloctadecyl ammonium chloride, ii) the stabilization of the obtained QAC@h-BN NPs by mixing with an aqueous solution of sodium alginate, and iii) soaking the homemade PP ultrafine fiber nonwovens (diameter 1–4 μm) in the stabilized QAC@h-BN NPs dispersion and post-crosslinking by Ca(II) ions. The QAC@h-BN-modified PP layer was then sandwiched between an internal layer (a hydrophilic

nonwoven) and an external layer (hydrophobic PP nonwoven) to assemble the mask (**Figure 15**a). The content of the immobilized NPs layer could be easily controlled by changing the concentration of the suspension mixture. The filtration efficiency for commercial PP (diameter 4–10 μm) were around 92% which was increased to 94% for the homemade PP ultrafine fiber nonwovens and further increased to >99% after treating with QAC@h-BN NPs. At the same time, the thermal conductivity of PP was 0.12 W m^{-1} K^{-1} which by coating with QAC@h-BN NPs increased to 0.88 W m^{-1} K^{-1} with almost no change during five
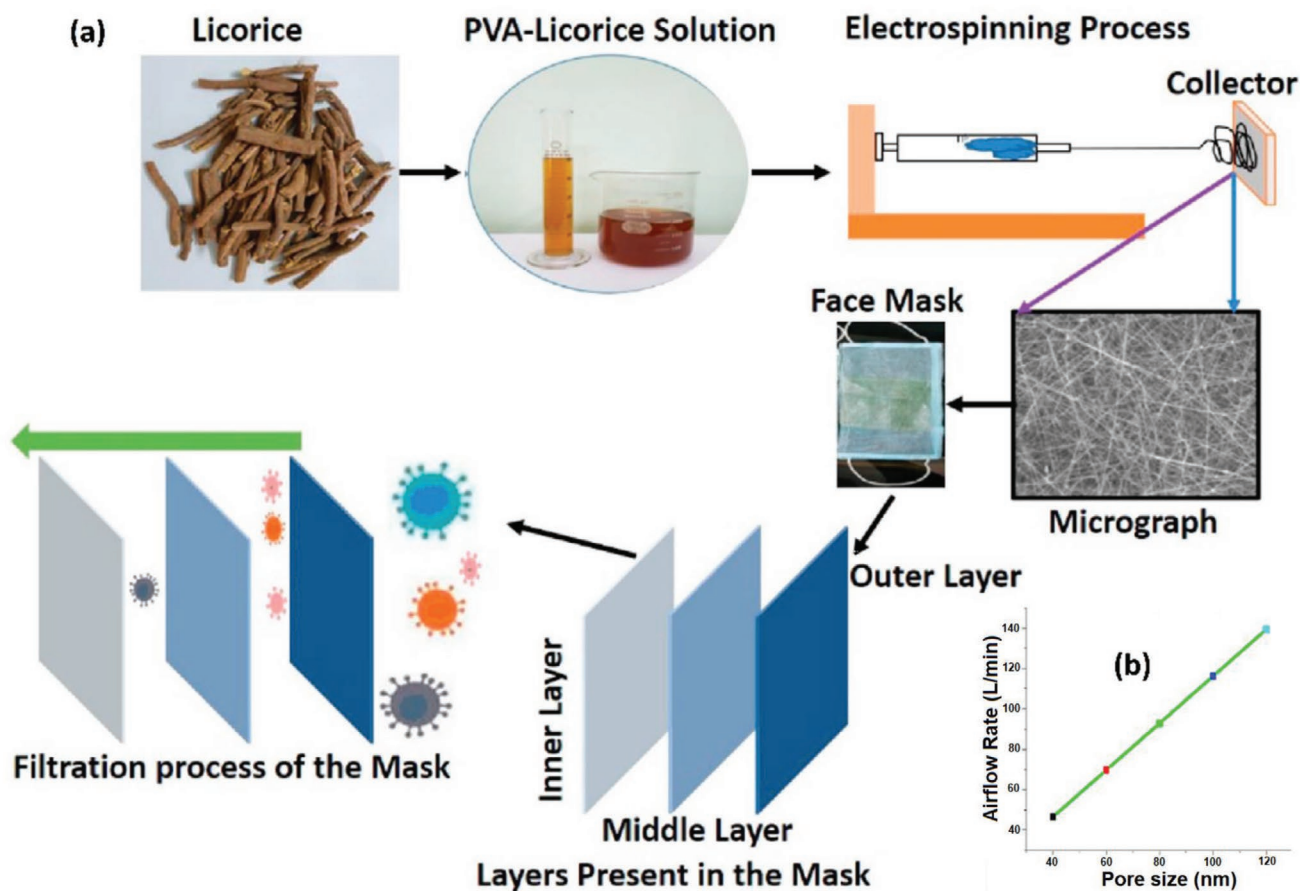
Figure 14. a) The electrospinning procedure of PVA/Licorice roots extracts for the fabrication of three-layer bio-based antiviral masks with nanofibrous structures. b) Airflow rate of the masks with different pore sizes. Reproduced with permission.[93] Copyright 2021, Elsevier.

times recycling (Figure 15b). The SEM images clearly showed the connection of the fibers by the NPs pastes (Figure 15c). While the unmodified PP layer showed almost no antibacterial activity, the QAC@h-BN/PP layer could kill >99% *E. coli* and 96% *S. aureus* (Figure 15d).

In another advanced strategy, a hybrid and reusable Cu/PAN-based filter composed of three layers was developed for potential application in face masks.[95] The three layers are shown in **Figure 16**b,c consist of i) the air filtration layer, made by the electrospinning of PAN solution in DMF, for the removal of airborne pollutants and particulate matter (PM), bacteria, or viruses from breathing stream, ii) the heating layer, made by electroplating of Cu on the PAN nanofiber mat, responsible for the production of high heat for deactivation of bacterial and virus particles, and iii) the thermal insulation layer made of polytetrafluoroethylene for preventing the heat from transferring to the other side of the filter and avoiding the burning of the human skin. This three-layer filter could be simply embedded into the structure of face masks to generate high local temperatures in response to weak voltages to kill the microorganisms (Figure 16d). The temperature increment responding to the voltage was directly related to the copper content which could be adjusted by the electroplating time. Exposing the 2 V voltage to the heating layer for 60 s, the temperatures were increased to 52, 100, and 133 °C for the samples with electroplating times

15, 30, and 60 s, respectively. Also, as depicted in Figure 16e,f increasing the applied voltage increased the temperature. The generated heat by the Cu microfiber mat could kill all the *E. coli* bacteria. Furthermore, the temperature and time required for deactivation of some viruses such as mouse hepatitis virus,[149] porcine epidemic diarrhea virus,[150] and SARS-CoV were below 60 °C and <30 min, suggesting the effectiveness of this filter under relatively moderate conditions.

Wang et al. prepared a rechargeable PVA-based mask with durable charge-retention even under high humid conditions.[96] The final mask was self-assembled by sandwiching the PVA fibers as the inner layer between two PP on the outer layers. The entire system acts as a TENG. Indeed, the PVA layer spontaneously forms H-bonding with H_2O molecules exhaled by the human body and fixes the water molecules which, therefore, increases the triboelectricity. This mask easily is rechargeable by hand touching. Additionally, friction between PVA and PP layer during breathing process can generate contact-charge and therefore, the fixed water molecules on PVA contribute to triboelectrification due to its high electropositivity. The overall result is the increase in the charge quantity of the medical mask. Compared to the PP-based TENG system, the performance of PVA-based TENG could be further enhanced by increasing the medium humidity. By increasing the humidity from 15% to 95%, the short-circuit current (I_{sc}) and open-circuit voltage (V_{oc}) were increased from
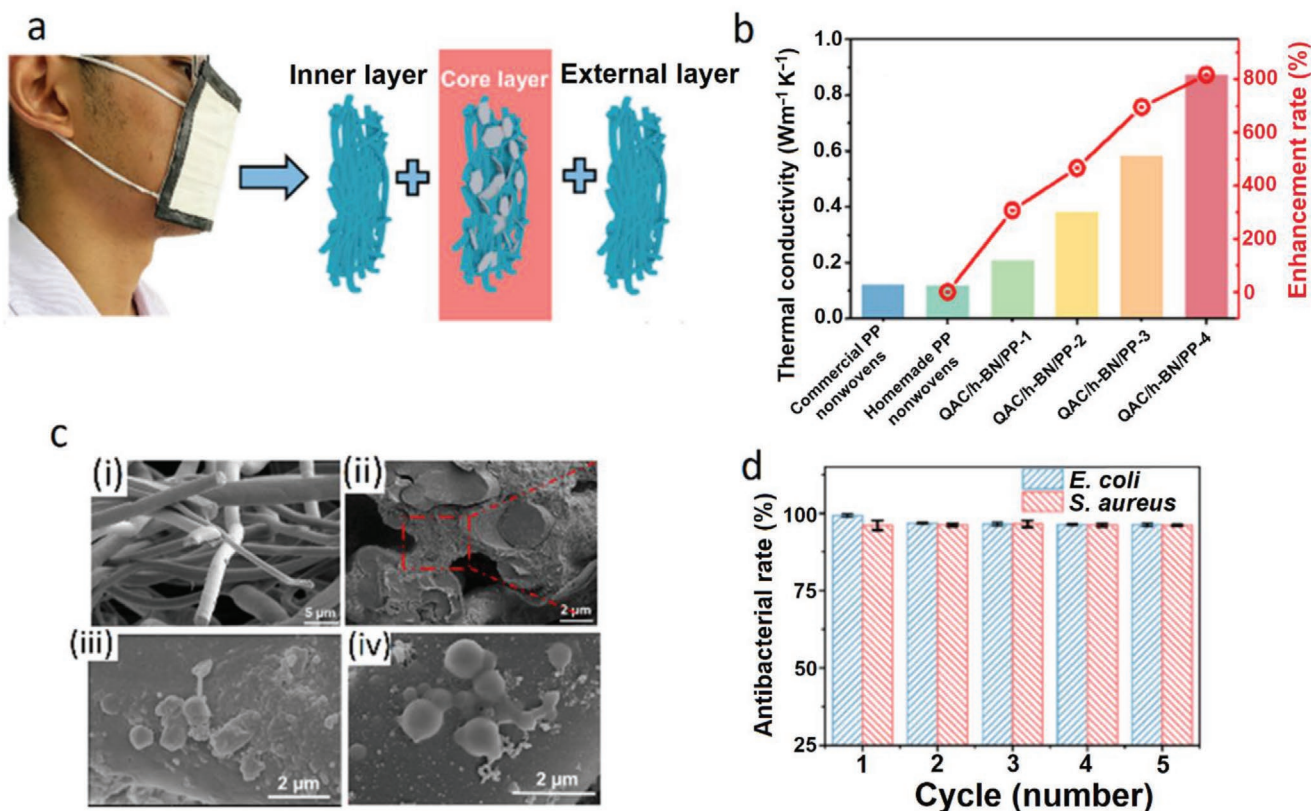
Figure 15. a) Schematic description for the assembly of the mask via sandwiching of the QAC@h-BN-modified PP layer between an internal layer (a hydrophilic nonwoven) and an external layer (hydrophobic PP nonwoven). b) Comparison of the thermal conductivity of the commercial PP nonwoven, homemade PP ultrafine fiber nonwoven, and QAC@h-BN-modified PP bearing different amounts of QAC@h-BN. c) SEM images of i) homemade PP ultrafine fiber, ii) QAC@h-BN/PP fibers, iii) killed *E. coli*, and iv) killed *S. aureus* cells on the QAC@h-BN/PP fibers. d) Antibacterial efficiencies of the QAC@h-BN/PP nanocomposite fibrous membranes after five times recycling. Reproduced with permission.[94] Copyright 2021, American Chemical Society.

14.4 µA and 220 V to 46.6 µA and 800 V, respectively, i.e., ≈26 times higher than those for PP TENG at 95% humidity. Therefore, despite the lack of antiviral results, this unique mask made from commodity polymers has good potential to prevent viral infection even in high-humidity environments.

5. Conclusion and Outlook

The fragility of the current face masks against COVID-19 highlighted the urgent demand for developing advanced and functionalized masks in the current or even postpandemics. The conventional masks only act as filtrating materials or barriers without deactivating viruses and bacteria. Consequently, the masks might become the sources for spreading viruses or microorganisms after disposal. Therefore, safe discarding methods are required to eliminate the spreading of this contaminated source. The most reliable method for discarding these masks is incineration. However, due to the production of over 250 000 tons of mask waste per day,[62] incineration generates a massive amount of toxic gases and CO_2, which raises pressing environmental concerns including the increase of greenhouse gases in the atmosphere. Accordingly, fabrication and development of functionalized masks with reusability, self-

sterilization, self-cleaning, antiviral, and antibacterial properties is in high demand to not only provide better protection against the pandemic diseases but also benefit the environment by reducing the excessive consumption of mask.

The addition of inherently antimicrobial agents such as metals (Ag, Cu, and Zn) and some types of essential oils has been proved as a versatile tool to boost the antiviral and antibacterial properties of the masks. The antimicrobial agents based on metal nanoparticles or ions rely on their steady and prolonged release from substrates (e.g., masks), followed by diffusing into the microorganism and destroying its DNA structure for deactivation. However, some types of metal ions such as Cu(II) and Zn(II) can create high cytotoxicity in high content upon contact with skin. Therefore, adjusting the content of metal ions at appropriate levels and proper fixation onto the mask to avoid the burst release is essential to reduce the side effects. On the other hand, the compounds releasing ROS as powerful antimicrobial agents can be fixed on the surface of mask layers by either covalent bonding or multi-electrostatic interactions. The release of ROS is often triggered by light irradiations. While these masks are highly efficient in daylight conditions, maintaining their effectiveness in dark environment is still challenging due to the failure or inability to release ROS. Therefore, further research on the incorporation of dark-active
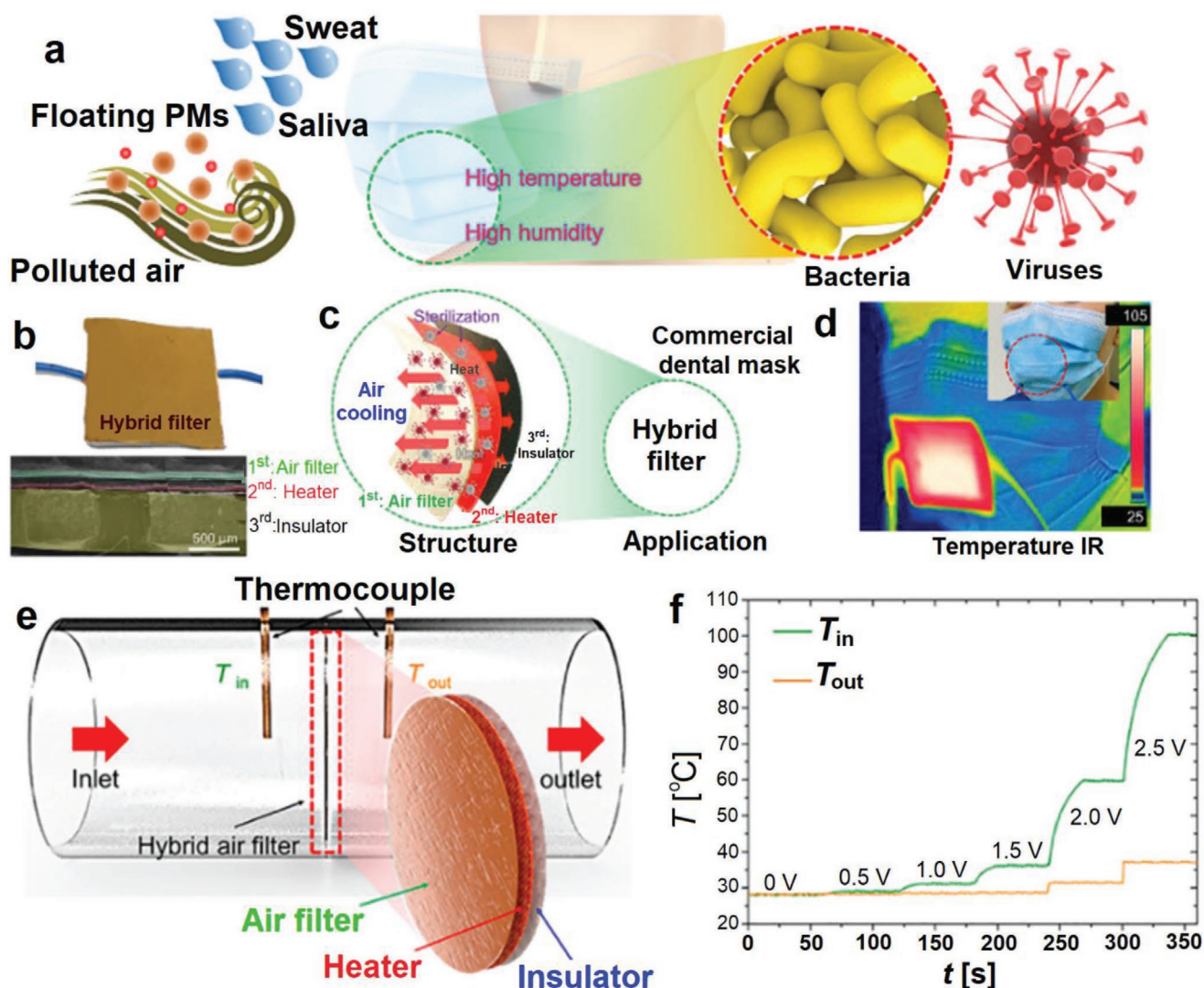
ADVANCED
SCIENCE NEWS
www.advancedsciencenews.com

NANO · MICRO
small
www.small-journal.com

Figure 16. a) The overall illustration of the common face masks that are exposing to PMs, bacteria and viruses from the saliva and sweat of humans. b) Photograph and a cross-section SEM image of the hybrid three-layer filer. c) Simple description of the rule of each later. d) Embedding this three-layer filter in a commercial facemask and recording the infrared image after applying a voltage of 3 V. e) Step for the filtration experiments and determination of the heating and insulation effectiveness of each layer in a layer in the hybrid filter. f) The heating and insulation performance of the hybrid layer. Reproduced with permission.[95] Copyright 2021, American Chemical Society.

ROS releasing compounds into the structure of the masks is required to provide a proper solution for this issue.

Many of the microorganisms can be deactivated upon heating. Indeed, the SARS-CoV-2 can be deactivated at 56 °C in 15 min.[151,152] Therefore, the addition of various agents to the masks that can create high local temperatures was introduced by several researchers. Among them, graphene is one of the best candidates since it not only possesses high electrothermal and photothermal properties but also can endow the masks with self-cleaning function due to its superhydrophobicity. The emerging technologies such as laser-induced forward transfer have been adopted for scaling-up the surface coating of the masks with thin graphene layers. Upon applying low voltages (<3 V) or sun illumination the temperature of the graphene layer can increase rapidly even to over 100 °C, which is far beyond the level required for inactivating various microorganisms

or viruses including SARS-CoV-2. Furthermore, a combination of other agents such as Ag or PVDF can further improve the antibacterial behavior and hydrophobicity of graphene-incorporated layers. However, Canada healthcare in a preliminary assessment has found that graphene nanoparticles can be inhaled by the mask wearers and therefore, create serious health risks, especially on lung.[153]

Another aspect that affects the performance of the surgical and N95 masks especially regarding the microorganism filtrations is the electrostatic charge that can adsorb or capture the microbes, thus inhibiting their transmittance to our breathing system. Incorporating TENGs between the friction layers of the masks has been utilized as a promising strategy to enhance the lifetime of electrostatic charges and endow the rechargeability of the masks upon simple friction movements of the masks such as by hand tapping or inhalation/exhalation breathing.

Despite significant advances that have been reported during last year in the fabrication of advanced face masks, by precise examining of the methods and strategies mentioned above, there are some challenges in practical applications of these as-fabricated face masks. i) Most of the developed methods require an external stimulus (such as light, voltage, and pressure) to trigger the functions of the incorporated active components, which practically limits the applications to some extent. For instance, those requiring light will not be useful in dark environments; whereas the functional agents requiring voltage to activate often rely on a battery carried by users, thus creating complication or inconvenient applications. ii) Instability or poor retention of the water-soluble modifying agents (such as inorganic salts, essential oils, and quaternary ammonium compounds) can be considered as the second significant issue. Therefore, fixation of such modifiers via various approaches for the controlled release of modifiers or the elimination of leaching-out of active components needs to be further explored. iii) While techniques based on the incorporation of nanomaterials into the structure of masks have been proved as promising for improving the antiviral activity of the masks, however, the possible inhaling of nanoparticles and therefore, generating toxicity is a great concern that needs to be addressed. iv) The majority of the modifications have been performed so far on PP-based nonwoven fabric which is non-biodegradable and has already created enormous environmental concerns after disposal; hence, the biodegradable fabrics possessing functions similar to PP are in high demand.

Overall, there are still plenty of rooms to further improve the properties and functions of the masks. On the one hand, replacing the PP nonwoven with cotton or cellulose-based nonwoven fabrics can reduce the environmental impact remarkably though the inherent features of PP nonwoven should be well maintained. On the other hand, the high hydrophilicity of the cotton or cellulose-based fabrics might reduce the self-cleaning properties of the masks. Therefore, the tailor-modification of those biodegradable fabrics is required. Accordingly, in our view, achieving an antiviral mask without creating health risks and environmental pollution is possible by fabrication of a multilayer mask based on the functionalized cotton or cellulose-based nonwovens: i) the outer and inner layers of the mask can be made by hydrophobization of the cellulose-based nonwoven grafted with hydrophobic chains or segments to improve the self-cleanliness of the mask; ii) the middle layer can be tailored by covalently grafting well-known biocompatible antiviral agents or polymers (such as aminoglycosides, polysaccharides,[154,155] peptides,[156] branched polymers and dendrimers,[157] etc.). The covalent grafting prevents the potential leaching of the ingredient via inhalation. Additionally, these masks tend to be washable and reusable easily. However, the feasibility of incorporating those polymers into the masks needs to be further assessed.

Acknowledgements

Conflict of Interest

The authors declare no conflict of interest.

Keywords

[1] N. Zhu, D. Zhang, W. Wang, X. Li, B. Yang, J. Song, X. Zhao, B. Huang, W. Shi, R. Lu, *N. Engl. J. Med.* **2020**, *382*, 727.

[2] C. Huang, Y. Wang, X. Li, L. Ren, J. Zhao, Y. Hu, L. Zhang, G. Fan, J. Xu, X. Gu, *Lancet* **2020**, *395*, 497.

[3] L. T. Phan, T. V. Nguyen, Q. C. Luong, T. V. Nguyen, H. T. Nguyen, H. Q. Le, T. T. Nguyen, T. M. Cao, Q. D. Pham, *N. Engl. J. Med.* **2020**, *382*, 872.

[4] J. F.-W. Chan, S. Yuan, K.-H. Kok, K. K.-W. To, H. Chu, J. Yang, F. Xing, J. Liu, C. C.-Y. Yip, R. W.-S. Poon, H.-W. Tsoi, S. K.-F. Lo, K.-H. Chan, V. K.-M. Poon, W.-M. Chan, J. D. Ip, J.-P. Cai, V. C.-C. Cheng, H. Chen, C. K.-M. Hui, K.-Y. Yuen, *Lancet* **2020**, *395*, 514.

[5] M. Chinazzi, J. T. Davis, M. Ajelli, C. Gioannini, M. Litvinova, S. Merler, A. P. y Piontti, K. Mu, L. Rossi, K. Sun, *Science* **2020**, *368*, 395.

[6] H. Lau, V. Khosrawipour, P. Kocbach, A. Mikolajczyk, J. Schubert, J. Bania, T. Khosrawipour, *J. Travel Med.* **2020**, *27*, 1.

[7] M. Nicola, Z. Alsafi, C. Sohrabi, A. Kerwan, A. Al-Jabir, C. Iosifidis, M. Agha, R. Agha, *Int. J. Surg.* **2020**, *78*, 185.

[8] W. Van Lancker, Z. Parolin, *Lancet Public Health* **2020**, *5*, 243.

[9] M. D. Knoll, C. Wonodi, *Lancet* **2021**, *397*, 72.

[10] L. R. Baden, H. M. El Sahly, B. Essink, K. Kotloff, S. Frey, R. Novak, D. Diemert, S. A. Spector, N. Rouphael, C. B. Creech, J. McGettigan, S. Khetan, N. Segall, J. Solis, A. Brosz, C. Fierro, H. Schwartz, K. Neuzil, L. Corey, P. Gilbert, H. Janes, D. Follmann, M. Marovich, J. Mascola, L. Polakowski, J. Ledgerwood, B. S. Graham, H. Bennett, R. Pajon, C. Knightly, B. Leav, W. Deng, H. Zhou, S. Han, M. Ivarsson, J. Miller, T. Zaks, C. S. Group, *N. Engl. J. Med.* **2021**, *384*, 403.

[11] F. Amanat, F. Krammer, *Immunity* **2020**, *52*, 583.

[12] Q. Li, J. Wu, J. Nie, L. Zhang, H. Hao, S. Liu, C. Zhao, Q. Zhang, H. Liu, L. Nie, H. Qin, M. Wang, Q. Lu, X. Li, Q. Sun, J. Liu, L. Zhang, X. Li, W. Huang, Y. Wang, *Cell* **2020**, *182*, 1284.

[13] B. Korber, W. M. Fischer, S. Gnanakaran, H. Yoon, J. Theiler, W. Abfalterer, N. Hengartner, E. E. Giorgi, T. Bhattacharya, B. Foley, *Cell* **2020**, *182*, 812.

[14] N. H. Leung, D. K. Chu, E. Y. Shiu, K.-H. Chan, J. J. McDevitt, B. J. Hau, H.-L. Yen, Y. Li, D. K. Ip, J. M. Peiris, *Nat. Med.* **2020**, *26*, 676.

[15] S. E. Eikenberry, M. Mancuso, E. Iboi, T. Phan, K. Eikenberry, Y. Kuang, E. Kostelich, A. B. Gumel, *Infect. Dis. Model.* **2020**, *5*, 293.

[16] S. Feng, C. Shen, N. Xia, W. Song, M. Fan, B. J. Cowling, *Lancet Respir. Med.* **2020**, *8*, 434.

[17] J. J. Klemeš, Y. Van Fan, R. R. Tan, P. Jiang, *Renewable Sustainable Energy Rev.* **2020**, *127*, 109883.

[18] S. Jung, S. Lee, X. Dou, E. E. Kwon, *Chem. Eng. J.* **2021**, *405*, 126658.

[19] S. Dharmaraj, V. Ashokkumar, S. Hariharan, A. Manibharathi, P. L. Show, C. T. Chong, C. Ngamcharussrivichai, *Chemosphere* **2021**, *272*, 129601.

ADVANCED
SCIENCE NEWS

www.advancedsciencenews.com

NANO · MICRO
small

www.small-journal.com

[20] J. S. Smith, H. Hanseler, J. Welle, R. Rattray, M. Campbell, T. Brotherton, T. Moudgil, T. F. Pack, K. Wegmann, S. Jensen, *J. Clin. Transl. Res.* **2020**, *5*, 1.

[21] E. Oral, K. K. Wannomae, R. L. Connolly, J. A. Gardecki, H. M. Leung, O. K. Muratoglu, A. Griffiths, A. N. Honko, L. E. Avena, L. G. McKay, *MedRxiv* **2020**, https://doi.org/10.1101/2020.04.11.20062026.

[22] G. Ibáñez-Cervantes, J. C. Bravata-Alcántara, A. S. Nájera-Cortés, S. Meneses-Cruz, L. Delgado-Balbuena, C. Cruz-Cruz, E. M. Durán-Manuel, M. A. Cureño-Díaz, E. Gómez-Zamora, S. Chávez-Ocaña, O. Sosa-Hernández, A. Aguilar-Rojas, J. M. Bello-López, *Am. J. Infect. Control* **2020**, *48*, 1037.

[23] E. P. Manning, M. D. Stephens, S. Patel, S. Dufresne, B. Silver, P. Gerbarg, Z. Gerbarg, C. D. Cruz, L. Sharma, *MedRxiv* **2020**, https://doi.org/10.1101/2020.05.28.20097402.

[24] L. Anderegg, C. Meisenhelder, C. O. Ngooi, L. Liao, W. Xiao, S. Chu, Y. Cui, J. M. Doyle, *PLoS One* **2020**, *15*, 0234851.

[25] R. K. Campos, J. Jin, G. H. Rafael, M. Zhao, L. Liao, G. Simmons, S. Chu, S. C. Weaver, W. Chiu, Y. Cui, *ACS Nano* **2020**, *14*, 14017.

[26] Y. Xiang, Q. Song, W. Gu, *Am. J. Infect. Control* **2020**, *48*, 880.

[27] L. Liao, W. Xiao, M. Zhao, X. Yu, H. Wang, Q. Wang, S. Chu, Y. Cui, *ACS Nano* **2020**, *14*, 6348.

[28] E. Hossain, S. Bhadra, H. Jain, S. Das, A. Bhattacharya, S. Ghosh, D. Levine, *Phys. Fluids* **2020**, *32*, 093304.

[29] D. Kim, J.-Y. Lee, J.-S. Yang, J. W. Kim, V. N. Kim, H. Chang, *Cell* **2020**, *181*, 914.

[30] B. W. Neuman, G. Kiss, A. H. Kunding, D. Bhella, M. F. Baksh, S. Connelly, B. Droese, J. P. Klaus, S. Makino, S. G. Sawicki, S. G. Siddell, D. G. Stamou, I. A. Wilson, P. Kuhn, M. J. Buchmeier, *J. Struct. Biol.* **2011**, *174*, 11.

[31] C. Castaño-Rodriguez, J. M. Honrubia, J. Gutiérrez-Álvarez, M. L. DeDiego, J. L. Nieto-Torres, J. M. Jimenez-Guardeño, J. A. Regla-Nava, R. Fernandez-Delgado, C. Verdia-Báguena, M. Queralt-Martín, G. Kochan, S. Perlman, V. M. Aguilella, I. Sola, L. Enjuanes, *mBio* **2018**, *9*, 02325.

[32] J. Zhang, H. Zeng, J. Gu, H. Li, L. Zheng, Q. Zou, *Vaccines* **2020**, *8*, 153.

[33] G. Kampf, D. Todt, S. Pfaender, E. Steinmann, *J. Hosp. Infect.* **2020**, *104*, 246.

[34] S. M. Imani, L. Ladouceur, T. Marshall, R. Maclachlan, L. Soleymani, T. F. Didar, *ACS Nano* **2020**, *14*, 12341.

[35] M. Fernández-Raga, L. Díaz-Marugán, M. García, C. Bort, V. Fanjul, *Environ. Res.* **2021**, *192*, 110293.

[36] N. Van Doremalen, T. Bushmaker, D. H. Morris, M. G. Holbrook, A. Gamble, B. N. Williamson, A. Tamin, J. L. Harcourt, N. J. Thornburg, S. I. Gerber, *N. Engl. J. Med.* **2020**, *382*, 1564.

[37] S. E. Ronca, R. X. Sturdivant, K. L. Barr, D. Harris, *HERD: Health Environ. Res. Des. J.* **2021**, 1937586721991535.

[38] A. Shamsi, T. Mohammad, S. Anwar, S. Amani, M. S. Khan, F. M. Husain, M. T. Rehman, A. Islam, M. I. Hassan, *Int. J. Biol. Macromol.* **2021**, *177*, 1.

[39] M. H. Al-Sayah, *J. Water Health* **2020**, *18*, 843.

[40] Z. Sun, K. Ostrikov, *Sustainable Mater. Technol.* **2020**, *25*, 00203.

[41] B. Adhikari, N. Sahu, *ChemistrySelect* **2021**, *6*, 2010.

[42] G. McDonnell, A. D. Russell, *Clin. Microbiol. Rev.* **1999**, *12*, 147.

[43] S. J. Volkoff, T. J. Carlson, K. Leik, J. J. Smith, D. Graves, P. Dennis, T. Aris, D. Cuthbertson, A. Holmes, K. Craig, *Ozone: Sci. Eng.* **2020**, 1.

[44] T. Cutts, S. Kasloff, D. Safronetz, J. Krishnan, *J. Hosp. Infect.* **2021**, *109*, 82.

[45] B. Bayarri, A. Cruz-Alcalde, N. López-Vinent, M. M. Micó, C. Sans, *J. Hazard. Mater.* **2021**, *415*, 125658.

[46] M. Stawarz-Janeczek, A. Kryczyk-Poprawa, B. Muszyńska, W. Opoka, J. Pytko-Polończyk, *Eur. J. Dent.* **2021**, 1.

[47] M. Hosseini, A. W. H. Chin, S. Behzadinasab, L. L. M. Poon, W. A. Ducker, *ACS Appl. Mater. Interfaces* **2021**, *13*, 5919.

[48] E. Hutter, J. H. Fendler, *Adv. Mater.* **2004**, *16*, 1685.

[49] M.-C. Wu, A. R. Deokar, J.-H. Liao, P.-Y. Shih, Y.-C. Ling, *ACS Nano* **2013**, *7*, 1281.

[50] X. Huang, P. K. Jain, I. H. El-Sayed, M. A. El-Sayed, *Lasers Med. Sci.* **2008**, *23*, 217.

[51] S. Riddell, S. Goldie, A. Hill, D. Eagles, T. W. Drew, *Virol. J.* **2020**, *17*, 145.

[52] C. S. Thakur, B. K. Jha, B. Dong, J. D. Gupta, K. M. Silverman, H. Mao, H. Sawai, A. O. Nakamura, A. K. Banerjee, A. Gudkov, *Proc. Natl. Acad. Sci. USA* **2007**, *104*, 9585.

[53] M. D. Smith, J. C. Smith, *ChemRxiv* **2020**, https://doi.org/10.26434/chemrxiv.11871402.

[54] R. Cristescu, R. J. Narayan, D. B. Chrisey, *MRS Adv.* **2020**, *5*, 2839.

[55] Z. Sun, T. Liao, K. Liu, L. Jiang, J. H. Kim, S. X. Dou, *Small* **2014**, *10*, 3001.

[56] Y. Zhang, J. Mei, C. Yan, T. Liao, J. Bell, Z. Sun, *Adv. Mater.* **2020**, *32*, 1902806.

[57] M. C. Sportelli, M. Izzi, E. A. Kukushkina, S. I. Hossain, R. A. Picca, N. Ditaranto, N. Cioffi, *Nanomaterials* **2020**, *10*, 802.

[58] E. Ruiz-Hitzky, M. Darder, B. Wicklein, C. Ruiz-Garcia, R. Martín-Sampedro, G. Del Real, P. Aranda, *Adv. Healthcare Mater.* **2020**, *9*, 2000979.

[59] E. V. R. Campos, A. E. S. Pereira, J. L. de Oliveira, L. B. Carvalho, M. Guilger-Casagrande, R. de Lima, L. F. Fraceto, *J. Nanobiotechnol.* **2020**, *18*, 125.

[60] M. D. Shin, S. Shukla, Y. H. Chung, V. Beiss, S. K. Chan, O. A. Ortega-Rivera, D. M. Wirth, A. Chen, M. Sack, J. K. Pokorski, *Nat. Nanotechnol.* **2020**, *15*, 646.

[61] E. Atangana, A. Atangana, *Results Phys.* **2020**, *19*, 103425.

[62] M. Karmacharya, S. Kumar, O. Gulenko, Y.-K. Cho, *ACS Appl. Bio Mater.* **2021**, *4*, 3891.

[63] N. Karim, S. Afroj, K. Lloyd, L. C. Oaten, D. V. Andreeva, C. Carr, A. D. Farmery, I.-D. Kim, K. S. Novoselov, *ACS Nano* **2020**, *14*, 12313.

[64] C. M. Clase, E. L. Fu, A. Ashur, R. C. L. Beale, I. A. Clase, M. B. Dolovich, M. J. Jardine, M. Joseph, G. Kansiime, J. F. E. Mann, R. Pecoits-Filho, W. C. Winkelmayer, J. J. Carrero, *Mayo Clin. Proc.* **2020**, *95*, 2204.

[65] M. Zhao, L. Liao, W. Xiao, X. Yu, H. Wang, Q. Wang, Y. L. Lin, F. S. Kilinc-Balci, A. Price, L. Chu, M. C. Chu, S. Chu, Y. Cui, *Nano Lett.* **2020**, *20*, 5544.

[66] A. Tcharkhtchi, N. Abbasnezhad, M. Zarbini Seydani, N. Zirak, S. Farzaneh, M. Shirinbayan, *Bioact. Mater.* **2021**, *6*, 106.

[67] M. Bandi, *Proc. R. Soc. A* **2020**, *476*, 20200469.

[68] C. E. Rodriguez-Martinez, M. P. Sossa-Briceño, J. A. Cortés, *Am. J. Infect. Control* **2020**, *48*, 1520.

[69] W. Yim, D. Cheng, S. H. Patel, R. Kou, Y. S. Meng, J. V. Jokerst, *ACS Appl. Mater. Interfaces* **2020**, *12*, 54473.

[70] K. K. Li, A. M. Joussen, J. K. Kwan, D. H. Steel, *FFP3, FFP2, N95, Surgical Masks and Respirators: What Should We Be Wearing for Ophthalmic Surgery in the COVID-19 Pandemic?*, Springer, Berlin **2020**.

[71] F.-S. Quan, I. Rubino, S.-H. Lee, B. Koch, H.-J. Choi, *Sci. Rep.* **2017**, *7*, 1.

[72] I. Rubino, E. Oh, S. Han, S. Kaleem, A. Hornig, S.-H. Lee, H.-J. Kang, D.-H. Lee, K.-B. Chu, S. Kumaran, S. Armstrong, R. Lalani, S. Choudhry, C. I. Kim, F.-S. Quan, B. Jeon, H.-J. Choi, *Sci. Rep.* **2020**, *10*, 13875.

[73] Y. Li, P. Leung, L. Yao, Q. Song, E. Newton, *J. Hosp. Infect.* **2006**, *62*, 58.

[74] C. B. Hiragond, A. S. Kshirsagar, V. V. Dhapte, T. Khanna, P. Joshi, P. V. More, *Vacuum* **2018**, *156*, 475.

[75] D. Kharaghani, M. Q. Khan, A. Shahzad, Y. Inoue, T. Yamamoto, S. Rozet, Y. Tamada, I. S. Kim, *Nanomaterials* **2018**, *8*, 461.

[76] M. Hashmi, S. Ullah, I. S. Kim, *Curr. Res. Biotechnol.* **2019**, *1*, 1.

[77] S. Kumar, M. Karmacharya, S. R. Joshi, O. Gulenko, J. Park, G.-H. Kim, Y.-K. Cho, *Nano Lett.* **2021**, *21*, 337.

[78] V. Gopal, B. E. Nilsson-Payant, H. French, W.-s. Yung, M. Hardwick, A. te Velthuis, *bioRxiv* **2020**, https://doi.org/10.1101/2020.11.02.365833.

[79] A. Kumar, A. Sharma, Y. Chen, M. M. Jones, S. T. Vanyo, C. Li, M. B. Visser, S. D. Mahajan, R. K. Sharma, M. T. Swihart, *Adv. Funct. Mater.* **2020**, *31*, 2008054.

[80] F. A. Monge, P. Jagadesan, V. Bondu, P. L. Donabedian, L. Ista, E. Y. Chi, K. S. Schanze, D. G. Whitten, A. M. Kell, *ACS Appl. Mater. Interfaces* **2020**, *12*, 55688.

[81] P. Tang, Z. Zhang, A. Y. El-Moghazy, N. Wisuthiphaet, N. Nitin, G. Sun, *ACS Appl. Mater. Interfaces* **2020**, *12*, 49442.

[82] E. Horváth, L. Rossi, C. Mercier, C. Lehmann, A. Sienkiewicz, L. Forró, *Adv. Funct. Mater.* **2020**, *30*, 2004615.

[83] J. Zhao, B. Deng, M. Lv, J. Li, Y. Zhang, H. Jiang, C. Peng, J. Li, J. Shi, Q. Huang, *Adv. Healthcare Mater.* **2013**, *2*, 1259.

[84] F. De Maio, V. Palmieri, G. Babini, A. Augello, I. Palucci, G. Perini, A. Salustri, M. De Spirito, M. Sanguinetti, G. Delogu, *medRxiv* **2020**, https://doi.org/10.1101/2020.09.16.20194316.

[85] S. P. Figerez, S. Patra, G. Rajalakshmi, T. Narayanan, *Oxford Open Mater. Sci.* **2021**, *1*, 003.

[86] X. Shan, H. Zhang, C. Liu, L. Yu, Y. Di, X. Zhang, L. Dong, Z. Gan, *ACS Appl. Mater. Interfaces* **2020**, *12*, 56579.

[87] H. Zhong, Z. Zhu, J. Lin, C. F. Cheung, V. L. Lu, F. Yan, C.-Y. Chan, G. Li, *ACS Nano* **2020**, *14*, 6213.

[88] H. Zhong, Z. Zhu, P. You, J. Lin, C. F. Cheung, V. L. Lu, F. Yan, C.-Y. Chan, G. Li, *ACS Nano* **2020**, *14*, 8846.

[89] L. Huang, S. Xu, Z. Wang, K. Xue, J. Su, Y. Song, S. Chen, C. Zhu, B. Z. Tang, R. Ye, *ACS Nano* **2020**, *14*, 12045.

[90] Z. Lin, Z. Wang, X. Zhang, D. Diao, *Nano Res.* **2021**, *14*, 1110.

[91] S. S. Ray, Y.-I. Park, H. Park, S.-E. Nam, I.-C. Kim, Y.-N. Kwon, *Environ. Technol. Innovation* **2020**, *20*, 101093.

[92] M. Martí, A. Tuñón-Molina, F. L. Aachmann, Y. Muramoto, T. Noda, K. Takayama, Á. Serrano-Aroca, *Polymers* **2021**, *13*, 207.

[93] M. A. Chowdhury, M. B. A. Shuvho, M. A. Shahid, A. K. M. M. Haque, M. A. Kashem, S. S. Lam, H. C. Ong, M. A. Uddin, M. Mofijur, *Environ. Res.* **2021**, *192*, 110294.

[94] S.-W. Xiong, P.-g. Fu, Q. Zou, L.-y. Chen, M.-y. Jiang, P. Zhang, Z.-g. Wang, L.-s. Cui, H. Guo, J.-G. Gai, *ACS Appl. Mater. Interfaces* **2021**, *13*, 196.

[95] Y.-I. Kim, M.-W. Kim, S. An, A. L. Yarin, S. S. Yoon, *ACS Appl. Mater. Interfaces* **2021**, *13*, 857.

[96] N. Wang, Y. Feng, Y. Zheng, L. Zhang, M. Feng, X. Li, F. Zhou, D. Wang, *Adv. Funct. Mater.* **2021**, *31*, 2009172.

[97] Y. N. Slavin, J. Asnis, U. O. Hafeli, H. Bach, *J. Nanobiotechnol.* **2017**, *15*, 65.

[98] S. Chernousova, M. Epple, *Angew. Chem., Int. Ed.* **2013**, *52*, 1636.

[99] K. Zheng, M. I. Setyawati, D. T. Leong, J. Xie, *Coord. Chem. Rev.* **2018**, *357*, 1.

[100] G. Grass, C. Rensing, M. Solioz, *Appl. Environ. Microbiol.* **2011**, *77*, 1541.

[101] A. K. Chatterjee, R. Chakraborty, T. Basu, *Nanotechnology* **2014**, *25*, 135101.

[102] A. Sirelkhatim, S. Mahmud, A. Seeni, N. H. M. Kaus, L. C. Ann, S. K. M. Bakhori, H. Hasan, D. Mohamad, *Nano-Micro Lett.* **2015**, *7*, 219.

[103] S. A. Read, S. Obeid, C. Ahlenstiel, G. Ahlenstiel, *Adv. Nutr.* **2019**, *10*, 696.

[104] M. Wu, B. Ma, T. Pan, S. Chen, J. Sun, *Adv. Funct. Mater.* **2016**, *26*, 569.

[105] Y. Wei, S. Chen, Y. Lin, X. Yuan, L. Liu, *J. Mater. Chem. C* **2016**, *4*, 935.

[106] B. Subramanian, K. Anu Priya, S. Thanka Rajan, P. Dhandapani, M. Jayachandran, *Mater. Lett.* **2014**, *128*, 1.

[107] M. Ibănescu, V. Muşat, T. Textor, V. Badilita, B. Mahltig, *J. Alloys Compd.* **2014**, *610*, 244.

[108] F. Pilaquinga, J. Morey, M. Torres, R. Seqqat, M. d. l. N. Piña, *WIRES Nanomed. Nanobiotechnol.* **2021**, e1707.

[109] D. Bradley, *Mater. Today* **2020**, *40*, 2.

[110] B. C. Sousa, D. L. Cote, *MRS Adv.* **2020**, *5*, 2873.

[111] A. V. Skalny, L. Rink, O. P. Ajsuvakova, M. Aschner, V. A. Gritsenko, S. I. Alekseenko, A. A. Svistunov, D. Petrakis, D. A. Spandidos, J. Aaseth, A. Tsatsakis, A. A. Tinkov, *Int. J. Mol. Med.* **2020**, *46*, 17.

[112] D.-S. Zhou, N. Xu, L. Li, G. Ji, G. Xue, *J. Phys. Chem. B* **2003**, *107*, 2748.

[113] S. Panda, T. K. Rout, A. D. Prusty, P. M. Ajayan, S. Nayak, *Adv. Mater.* **2018**, *30*, 1702149.

[114] A. R. Patel, *Adv. Funct. Mater.* **2020**, *30*, 1806809.

[115] K. Midander, P. Cronholm, H. L. Karlsson, K. Elihn, L. Möller, C. Leygraf, I. O. Wallinder, *Small* **2009**, *5*, 389.

[116] M. Arens, S. Travis, *J. Clin. Microbiol.* **2000**, *38*, 1758.

[117] H. Xiao, Y. Song, G. Chen, *J. Electrost.* **2014**, *72*, 311.

[118] S. O. Aisida, N. Madubuonu, M. H. Alnasir, I. Ahmad, S. Botha, M. Maaza, F. I. Ezema, *Appl. Nanosci.* **2020**, *10*, 305.

[119] X. Gu, Z. Xu, L. Gu, H. Xu, F. Han, B. Chen, X. Pan, *Environ. Chem. Lett.* **2021**, *19*, 167.

[120] J. Lin, N.-Y. T. Nguyen, C. Zhang, A. Ha, H. H. Liu, *ACS Omega* **2020**, *5*, 24613.

[121] J. F. Lovell, T. W. B. Liu, J. Chen, G. Zheng, *Chem. Rev.* **2010**, *110*, 2839.

[122] K. Liu, Y. Liu, Y. Yao, H. Yuan, S. Wang, Z. Wang, X. Zhang, *Angew. Chem., Int. Ed.* **2013**, *52*, 8285.

[123] T. Zhou, R. Hu, L. Wang, Y. Qiu, G. Zhang, Q. Deng, H. Zhang, P. Yin, B. Situ, C. Zhan, A. Qin, B. Z. Tang, *Angew. Chem., Int. Ed.* **2020**, *59*, 9952.

[124] A. Hou, G. Feng, J. Zhuo, G. Sun, *ACS Appl. Mater. Interfaces* **2015**, *7*, 27918.

[125] S. Yi, S. Wu, Y. Zhang, Y. Zou, F. Dai, Y. Si, *ACS Sustainable Chem. Eng.* **2020**, *8*, 16775.

[126] A. Scheberl, M. L. Khalil, F. Maghsoodi, E. W. Strach, J. Yang, E. Y. Chi, K. S. Schanze, E. Reimhult, D. G. Whitten, *ACS Appl. Mater. Interfaces* **2020**, *12*, 21322.

[127] Y. Nosaka, A. Y. Nosaka, *Chem. Rev.* **2017**, *117*, 11302.

[128] P. Ribao, J. Corredor, M. J. Rivero, I. Ortiz, *J. Hazard. Mater.* **2019**, *372*, 45.

[129] Y. Tong, G. Shi, G. Hu, X. Hu, L. Han, X. Xie, Y. Xu, R. Zhang, J. Sun, J. Zhong, *Chem. Eng. J.* **2021**, *414*, 128788.

[130] V. Kumaravel, K. M. Nair, S. Mathew, J. Bartlett, J. E. Kennedy, H. G. Manning, B. J. Whelan, N. S. Leyland, S. C. Pillai, *Chem. Eng. J.* **2021**, 129071.

[131] L. Rossi, R. Foschia, A. Glushkova, L. Forró, E. Horváth, *Ceram. Int.* **2020**, *46*, 17729.

[132] X. Li, N. Kwon, T. Guo, Z. Liu, J. Yoon, *Angew. Chem., Int. Ed.* **2018**, *57*, 11522.

[133] Y. Jing, Q. Xu, M. Chen, X. Shao, *Bioorg. Med. Chem.* **2019**, *27*, 2201.

[134] W. Hu, C. Peng, W. Luo, M. Lv, X. Li, D. Li, Q. Huang, C. Fan, *ACS Nano* **2010**, *4*, 4317.

[135] S. Liu, T. H. Zeng, M. Hofmann, E. Burcombe, J. Wei, R. Jiang, J. Kong, Y. Chen, *ACS Nano* **2011**, *5*, 6971.

[136] J. Zhu, J. Wang, J. Hou, Y. Zhang, J. Liu, B. Van der Bruggen, *J. Mater. Chem. A* **2017**, *5*, 6776.

[137] V. Palmieri, M. Papi, *Nano Today* **2020**, *33*, 100883.

[138] G. Reina, D. Iglesias, P. Samori, A. Bianco, *Adv. Mater.* **2021**, *33*, 2007847.

[139] I. S. Donskyi, C. Nie, K. Ludwig, J. Trimpert, R. Ahmed, E. Quaas, K. Achazi, J. Radnik, M. Adeli, R. Haag, K. Osterrieder, *Small* **2021**, *17*, 2007091.

[140] J. Lee, J. Kim, *Polymers* **2020**, *12*, 721.

[141] P. Lv, L. Shi, C. Fan, Y. Gao, A. Yang, X. Wang, S. Ding, M. Rong, *ACS Appl. Mater. Interfaces* **2020**, *12*, 15012.

[142] G. Li, *J. Appl. Phys.* **2020**, *127*, 010901.

[143] Y. Li, D. X. Luong, J. Zhang, Y. R. Tarkunde, C. Kittrell, F. Sargunaraj, Y. Ji, C. J. Arnusch, J. M. Tour, *Adv. Mater.* **2017**, *29*, 1700496.

[144] N. Jiang, Y. Wang, K. C. Chan, C.-Y. Chan, H. Sun, G. Li, *Global Challenges* **2020**, *4*, 1900054.

[145] A. W. H. Chin, J. T. S. Chu, M. R. A. Perera, K. P. Y. Hui, H.-L. Yen, M. C. W. Chan, M. Peiris, L. L. M. Poon, *Lancet Microbe* **2020**, *1*, e10.

[146] J. Lin, Z. Peng, Y. Liu, F. Ruiz-Zepeda, R. Ye, E. L. Samuel, M. J. Yacaman, B. I. Yakobson, J. M. Tour, *Nat. Commun.* **2014**, *5*, 1.

[147] J. Cinatl, B. Morgenstern, G. Bauer, P. Chandra, H. Rabenau, H. Doerr, *Lancet* **2003**, *361*, 2045.

[148] S. Ji, Z. Li, W. Song, Y. Wang, W. Liang, K. Li, S. Tang, Q. Wang, X. Qiao, D. Zhou, S. Yu, M. Ye, *J. Nat. Prod.* **2016**, *79*, 281.

[149] M. Saknimit, I. Inatsuki, Y. Sugiyama, K.-i. Yagami, *Exp. Anim.* **1988**, *37*, 341.

[150] M. M. Hulst, L. Heres, R. W. Hakze-van der Honing, M. Pelser, M. Fox, W. H. M. van der Poel, *J. Appl. Microbiol.* **2019**, *126*, 1931.

[151] P. Yang, X. Wang, *Cell. Mol. Immunol.* **2020**, *17*, 555.

[152] P. Zhou, X.-L. Yang, X.-G. Wang, B. Hu, L. Zhang, W. Zhang, H.-R. Si, Y. Zhu, B. Li, C.-L. Huang, *Nature* **2020**, *579*, 270.

[153] H. Jackson, https://globalnews.ca/news/7736862/mask-recall-graphene/ (accessed: April 2021).

[154] L. Chen, G. Huang, *Int. J. Biol. Macromol.* **2018**, *115*, 77.

[155] X. He, J. Fang, Q. Guo, M. Wang, Y. Li, Y. Meng, L. Huang, *Carbohydr. Polym.* **2020**, *229*, 115548.

[156] L. C. Pereira Vilas Boas, M. L. Campos, R. L. Araujo Berlanda, N. d. C. Neves, O. L. Franco, *Cell. Mol. Life Sci.* **2019**, *76*, 3525.

[157] R. H. Bianculli, J. D. Mase, M. D. Schulz, *Macromolecules* **2020**, *53*, 9158.

Farzad Seidi obtained his Ph.D. in the polymer chemistry laboratory at the Sharif University of Technology in 2011. In 2016, he joined the new established Vidyasirimedhi Institute of Science and Technology (VISTEC) in Thailand as a team leader in the research group of Prof. Daniel Crespy. Since 2019, Dr. Seidi is working as an associate professor in Nanjing Forestry University in China. To date, he has published 90 ISC peer-reviewed journal papers. His research interests are mainly focusing on the chemical fabrication of functional polymers and modification of biopolymers to generate innovative traits for both biomedical and industrial applications.

Huining Xiao, a professor in Chemical Engineering at University of New Brunswick (UNB) and the Fellow of Canadian Academy of Engineering, obtained his Ph.D. in Chemical Engineering at McMaster University in Canada in 1995. Before joining the UNB in 2001, he was a lecturer at the University of Manchester in the UK from 1996 to 2001. To date Dr. Xiao has published over 300 peer-reviewed journal papers. His key research interests include responsive polymers and hydrogels as drug carriers or vectors for gene delivery, functional-modified cellulose fibers, antimicrobial polymers and nanoparticles, bioadsorbent and bionanocomposites, barrier-enhanced green packaging, and cellulosic foam materials.